
Understanding the effects of carbon and stainless steel fibers on electrical and mechanical properties on selected engineering thermoplastics (PA6 and PBT)

Auteur : Abdi Alin, Gaël

Promoteur(s) : 2526

Faculté : Faculté des Sciences

Diplôme : Master en sciences chimiques, à finalité approfondie

Année académique : 2016-2017

URI/URL : <http://hdl.handle.net/2268.2/2490>

Avertissement à l'attention des usagers :

Tous les documents placés en accès ouvert sur le site le site MatheO sont protégés par le droit d'auteur. Conformément aux principes énoncés par la "Budapest Open Access Initiative"(BOAI, 2002), l'utilisateur du site peut lire, télécharger, copier, transmettre, imprimer, chercher ou faire un lien vers le texte intégral de ces documents, les disséquer pour les indexer, s'en servir de données pour un logiciel, ou s'en servir à toute autre fin légale (ou prévue par la réglementation relative au droit d'auteur). Toute utilisation du document à des fins commerciales est strictement interdite.

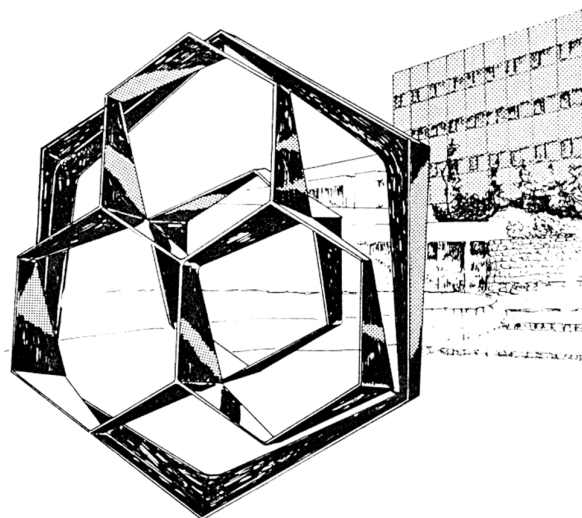
Par ailleurs, l'utilisateur s'engage à respecter les droits moraux de l'auteur, principalement le droit à l'intégrité de l'oeuvre et le droit de paternité et ce dans toute utilisation que l'utilisateur entreprend. Ainsi, à titre d'exemple, lorsqu'il reproduira un document par extrait ou dans son intégralité, l'utilisateur citera de manière complète les sources telles que mentionnées ci-dessus. Toute utilisation non explicitement autorisée ci-avant (telle que par exemple, la modification du document ou son résumé) nécessite l'autorisation préalable et expresse des auteurs ou de leurs ayants droit.



Faculty of Sciences
Chemistry Department

Centre for Education and Research on Macromolecules (CERM)
Prof. Christine JEROME

Understanding the effects of carbon and
stainless steel fibers on electrical and
mechanical properties on selected
engineering thermoplastics (PA6 and PBT)



Academic year 2016-2017

Dissertation presented by
Gaël ABDI ALIN
In partial fulfillment
of the requirements for the degree
Master of Chemical Sciences

Foreword

This thesis marks the end of years of heavy, theoretical courses at the University of Liège. Hereby, are presented the results of 5 months of hard work that wouldn't have been possible without all the support I had all along this project and I would like to take this opportunity to thank some people.

First of all, I would like to thank my parents for allowing me to start my studies and all their support during these sometimes difficult years.

I also want to express my heartfelt thanks to my girlfriend, Adeline, for her constant support and all her good cares during all my studies and this master thesis. I know it wasn't always easy, especially near the end.

I would like to thank everyone that has participated in this project. Firstly, my supervisors Santiago Pierre and Christine Jérôme for their support throughout this project and taking the time to correct my thesis.

I also thank all the people at the Cabot Application Development Center in Pepinster for the warm welcome received. Especially, I express all my gratitude to Benjamin Goessens, for his kindness during all these hours spent with me on the APV and his awesome committed technical support all along this project.

I very warmly thank Sebastien Delperdange for his precious help during injection molding and Marc Nyssen for his support and advices at the analytical laboratory.

Lastly, I also express all my consideration to people that are not mentioned here involved in any way in this project.

Gaël Abdi Alin

Table of Contents

1. General	1
1.1. Motivation	1
1.2. Project objectives	3
2. Theoretical background	4
2.1. Electrical properties of conductive composites	4
▪ Percolation phenomenon.....	4
▪ Electrical conduction mechanisms.....	6
2.2. Material selection	8
▪ Carbon black (CB).....	9
▪ Short fibers	11
▪ Stainless steel fiber.....	12
▪ Carbon fiber	14
2.3. Mechanics of short fiber reinforced polymers	21
▪ Critical fiber length (L_c)	22
▪ Surface treatments and sizing	24
▪ Rule of mixture (RoM) for mechanical properties prediction in composites	25
2.4. Fiber compounding.....	28
2.5. Hybridization.....	30
3. Materials and methods	32
3.1. Materials.....	32
3.2. Samples preparation.....	33
▪ Twin-Screw compounding.....	33
▪ Injection molding	34
3.3. Characterization techniques.....	35
▪ Fiber lengths.....	35
▪ Volume resistivity.....	37
▪ Tensile properties	38
▪ Flexural strength	39
▪ Notched impact resistance.....	40
▪ Scanning Electron Microscopy (SEM).....	41
4. Results and discussions	42
4.1. Twin screw extrusion (TSE) compounding optimization.....	43

▪ Influence of screw speed on residual length of fibers	44
▪ Influence of output rate on residual length of fibers	46
▪ Influence of temperature on residual length of fibers	47
▪ Influence of loading on residual length of fibers	48
▪ Conclusion	48
4.2. Electrical and mechanical properties of composites.....	49
▪ Volume resistivity.....	49
▪ Yield strength.....	54
▪ Flexural strength.....	60
▪ Elastic modulus.....	61
▪ Notched impact resistance.....	62
4.3. Hybrid composite	65
▪ Stainless steel fiber (SF) – carbon fiber (CF) hybrid.....	66
▪ Conclusion	72
▪ Carbon black (CB) – carbon fiber (CF) hybrid	73
▪ Conclusion	77
5. Conclusion and perspectives	77
Annexes.....	81
▪ A-1: Popular fillers and application.....	81
▪ A-2: Datasheets.....	82
▪ A-3: Profile screw configuration	87
▪ A-4: Compounding parameters and samples composition.....	89
Bibliographic references.....	96

Abstract

Cabot Corporation supplies a broad range of carbon black based electrically conductive composites (CABELEC®) which are widely used in the automotive, electronics and electrical packaging and equipment industry. Nowadays, the demand in high performance conductive compounds is increasing but carbon black however provides only moderate reinforcements in mechanical properties. Within this framework, the purpose of this project was to provide a comprehensive understanding of the effects of carbon fiber (PAN and PITCH) and stainless steel fibers toward performances of polyamide 6 based composite. In this work, composites were compounded by twin screw extrusion. Since fibers aspect ratio is of crucial importance to manufacture good performance composite, the first part of this project was dedicated to the evaluation and optimization of compounding settings in order to maximize fibers aspect ratio. Increasing screw speed and filler loading enhanced fibers degradation whereas higher output rate and temperature displayed significant impact on preserving fibers. In the second part, the effects of selected fillers toward electrical (i.e. volume resistivity) and mechanical (strength, stiffness and toughness) properties were thoroughly investigated. Carbon fiber PAN, owing its lower degradation during compounding and better adhesion to the polymeric matrix used, appears to be the more efficient in providing conductivity (i.e. volume resistivity of 10 Ohm.cm and percolation at 3.4% vol.) and reinforcements. In the last part, hybrids (i.e. containing at least two different fillers) were investigated. The first hybrid, containing stainless steel and carbon PAN fibers, displayed synergistic effects toward electrical properties and good mechanical performance although mechanical enhancement was lower than expected assumedly due to higher shear during compounding by fiber-fiber interactions. Lastly, hybrid containing mostly carbon black and small amount of carbon PAN fibers (i.e. 2% wt.) was investigated. Carbon fibers in such hybrids provided enhanced electrical properties and effective reinforcement in term of strength (+15%) and stiffness (+20%).

List of figures and tables

List of figures

FIGURE 1 : PERCOLATION PHENOMENA SCHEME. ADAPTED FROM [1]	5
FIGURE 2 : INFLUENCE OF ASPECT RATIO ON PERCOLATION THRESHOLD [7]	7
FIGURE 3: CARBON BLACK PRIMARY PARTICLE CONSISTING OF CARBON COVALENTLY BONDED IN AN AMORPHOUS FORM. THE PRIMARY PARTICLE USUALLY PRESENTS A SPHERICAL SHAPE AND IS AROUND 50NM.[9].....	9
FIGURE 4 : FORMATION OF AGGLOMERATE A) PRIMARY PARTICLE MADE OF CARBON ATOM COVALENTLY BOND, B) AGGREGATE CONSISTING OF FUSED PRIMARY PARTICLE, C) AGGREGATE WEAKLY BOND TOGETHER BY VDW INTERACTION TO FORM AGGLOMERATE. [10]	10
FIGURE 5 : TRENDS AND FORECAST IN CARBON FIBER SHIPMENT.[8].....	14
FIGURE 6 : CARBON FIBER ILLUSTRATION REPRESENTING SHEETS INTERLOCKING AT DIFFERENT TEMPERATURE. IT SHOWS TRANSFORMATION OF CARBON STRUCTURE WITH TEMPERATURE: (A) AMORPHOUS (NON-CRYSTALLINE) AT 400 °C, (B) TURBOSTRATIC CRYSTALLITES AT 800 °C, AND (C) GRAPHENE SHEET STRUCTURE (GRAPHITE) DOMINANT ABOVE 1100 °C. [17]	15
FIGURE 7 : CARBON FIBERS CLASSIFICATION ACCORDING PRECURSORS USED DURING THE MANUFACTURING. PAN FIBERS ARE USUALLY STRONGER AND LESS STIFF WHEREAS PITCH FIBERS ARE STIFFER AND LESS STRONG.[19]	16
FIGURE 8 : STABILIZATION STEP IN CARBON FIBER PRODUCTION PROCESS. THE PAN FIBERS ARE HEATED AT 300°C AND THEIR CYANO SIDE GROUP REACT TOGETHER TO FORM STABLE CYCLIC RING.[20].....	17
FIGURE 9 : SECOND STEP OF STABILIZATION STEP IN CARBON FIBER PRODUCTION PROCESS. FIBERS ARE HEATED TO 700°C ALLOWING ELIMINATION OF H ₂ AND FORMATION OF AROMATIC PYRIDINE WHICH CAN FURTHER FUSED WITH OTHER CHAINS. [20]	17
FIGURE 10 : CARBONIZATION FIRST STEP: ELIMINATION OF REMAINING IMPURITIES AND FUSION OF ADJACENT CHAINS. THIS IS DONE BY FURTHER HEATING OF THE PREVIOUSLY OBTAINED AROMATIC PYRIDINE CHAINS. [20].....	18
FIGURE 11 : RIBBONS FUSED TOGETHER TO GIVE LARGER RIBBONS. EACH RIBBON CONTAIN CARBON IN ITS HEXAGONAL STRUCTURE [20]	19
FIGURE 12 : TURBOSTRATIC CARBON FIBERS: CARBON ARE HIGHLY ORDERED IN THE SHORT RANGE BUT NOT AT HIGHER RANGE [20]	19
FIGURE 13 : REPARTITION OF THE LOAD ALONG FIBER AXIS. STRESS IS MAXIMAL IN THE MIDDLE AND MINIMUM AT THE ENDS. WHEN THE FIBER IS SHORTER THAN THE CRITICAL LENGTH, THE APPLIED STRAIN IS NOT TOTALLY TRANSFERRED TO THE FIBER AND MATRIX MAY FRACTURE BEFORE FIBERS (<i>l</i> ₁). AT THE CRITICAL LENGTH, THE LOAD IS EFFECTIVELY TRANSFER. CONSEQUENTLY, FIBERS AND MATRIX FAIL AT THE SAME STAIN AND THE COMPOSITE IS EFFECTIVELY REINFORCED (<i>l</i> _c). BEYOND THE CRITICAL LENGTH, THE FIBERS WILL CARRY AN GROWING FRACTION OF THE APPLIED LOAD (<i>l</i> ₂).[21].	23
FIGURE 14: EFFECTS OF FIBER ORIENTATION ON TENSILE MODULUS OF CARBON FIBER REINFORCED EPOXY RESINS.[25].....	25
FIGURE 15: LENGTH CORRECTION FACTOR CORRELATION WITH FIBER LENGTH APPLIED FOR GLASS FIBER REINFORCED EPOXY RESIN. ADAPTED FROM [25].....	26
FIGURE 16: TWIN SCREW EXTRUDER: SCHEMATIC APPARATUS [27]	29
FIGURE 17: HYBRID COMPOSITES USUALLY FOLLOW A RULE OF MIXTURE. DEVIATION FROM THIS RULE MAY BE OBSERVED WHEN POSITIVE (SYNERGISTIC) OR NEGATIVE HYBRID EFFECTS OCCUR. ADAPTED FROM [25].....	30
FIGURE 18: APV MP30AC 40:1 ILLUSTRATION OF MAIN PARTS (I.E. BARREL, DYE, COOLING BATH AND SIDE FEEDER)	33

FIGURE 19: INJECTION MOLDING MACHINE SCHEMATIC APPARATUS. PELLETS ARE FED BY A HOPPER INTO A HEATED BARREL THAT MIXES AND INJECTS MELTED MATERIALS INTO A MOLD. [28].....	34
FIGURE 20: LEICA DMLM OPTICAL MICROSCOPE AND RELATED LEICA DFC295 CAMERA.....	35
FIGURE 21: IMAGE ANALYSIS PROCESS.....	36
FIGURE 22: STRESS - STRAIN CURVES AND RELATED PROPERTIES. [29].....	38
FIGURE 23: THREE POINT BENDING FLEXURAL TEST. [30].....	39
FIGURE 24: BARS AND NOTCHES SIZE.....	40
FIGURE 25: SCANNING ELECTRON MICROSCOPE PRINCIPLE ILLUSTRATION. [32].....	41
FIGURE 26: RESULTS STRUCTURE PLAN.....	42
FIGURE 27: INFLUENCE OF SCREW SPEED ON RESIDUAL LENGTH OF CARBON FIBERS.....	44
FIGURE 28: SHEAR THINNING PHENOMENON ILLUSTRATION [34].....	45
FIGURE 29: INFLUENCE OF THROUGHPUT ON RESIDUAL LENGTH OF CARBON FIBER.....	46
FIGURE 30: INFLUENCE OF TEMPERATURE ON RESIDUAL LENGTH OF CARBON FIBERS.....	47
FIGURE 31: INFLUENCE OF LOADING ON RESIDUAL LENGTH OF CARBON FIBERS.....	48
FIGURE 32: DEPENDENCE OF VOLUME RESISTIVITY ON THE FILLER CONTENT IN POLYAMIDE 6.....	49
FIGURE 33: SCANNING ELECTRON MICROSCOPY OF RAW STAINLESS STEEL FIBERS (LEFT) AND CARBON FIBERS PAN (RIGHT). STAINLESS STEEL HIGH SIZING AMOUNT CAN BE SEEN BY THE LESS NEAT SURFACE THEY EXHIBIT WHEN COMPARED TO CARBON FIBERS.....	50
FIGURE 34: COMPARISON OF STAINLESS STEEL, PITCH CARBON FIBERS AND PAN CARBON FIBERS LENGTHS. SAMPLES WERE PREPARED USING THE SAME OPTIMIZED COMPOUNDING CONDITIONS AND 15% WT. IN PA6.....	51
FIGURE 35: PERCOLATION CURVES OF CARBON FIBERS PAN AND STAINLESS STEEL FIBERS IN PBT AND PA6 USING OPTIMIZED COMPOUNDING SETTINGS.....	52
FIGURE 36: MELT FLOW INDEX (VISCOSITY) COMPARISON BETWEEN PBT AND PA6. PBT EXHIBITS MUCH LOWER VISCOSITY (HIGHER MFI) THAN PA6. TESTS WERE PERFORMED AT 250°C AND 10KG LOADING.....	53
FIGURE 37: COMPARISON BETWEEN CARBON FIBERS LENGTH IN PA6 AND PBT. IT IS OBSERVED THAT CARBON FIBERS EXHIBIT HIGHER LENGTH ESPECIALLY AT HIGHER LOADING.....	53
FIGURE 38: INFLUENCE OF FILLER NATURES AND CONTENT ON YIELD STRENGTH OF PA6.....	54
FIGURE 39: SCANNING ELECTRON MICROSCOPY PICTURE OF A FRACTURED COMPOSITE MADE OF 15%WT. STAINLESS STEEL FIBERS IN PA6.....	55
FIGURE 40: SCHEMATIC REPRESENTATION OF FIBER ORIENTATION IN COMPOSITE. FIBERS CAN EITHER ORIENT RANDOMLY, RANDOMLY (IN PLANE) OR UNIDIRECTIONALLY [38].....	56
FIGURE 41: OPTICAL MICROGRAPH OF SAMPLE CONTAINING 10%WT. CARBON FIBERS PAN IN PA6.....	57
FIGURE 42: COMPARISON BETWEEN COMPUTED VALUES OBTAINED FROM THE ROM AND EXPERIMENTAL DATA.....	58
FIGURE 43: INFLUENCE OF MATRIX TOWARD YIELD STRENGTH.....	59
FIGURE 44: INFLUENCE OF FILLER LOADING AND NATURE ON FLEXURAL STRENGTH OF PA6 AND PBT.....	60
FIGURE 45 : INFLUENCE OF FILLER LOADING (%WT.) AND NATURE ON ELASTIC MODULUS IN COMPOSITE (PA6 AND PBT).....	61
FIGURE 46: INFLUENCE OF FILLER NATURE AND LOADING ON IMPACT PROPERTIES OF COMPOSITE (PA6 AND PBT).....	62
FIGURE 47: THE MATRIX CRACK REACHES THE FIBER (A), DELAMINATION OCCURS (B), FIBER FRACTURE IS SHOWN IN (C) FOLLOWED BY FIBER PULLOUT IN (D). [38].....	63
FIGURE 48: DETAILED SCHEME REPRESENTING COMPLETE PULL-OUT MECHANISM.[39].....	64
FIGURE 49: STAINLESS STEEL FIBERS FRACTURED COMPOSITE WHERE COMPLETE FIBER PULL OUT OF PA6 MATRIX IS OBSERVED (LEFT).PAN CARBON FIBERS FRACTURED COMPOSITES WHERE A FIBER IS STILL STUCK INTO THE PA6 MATRIX AFTER RUPTURE. THIS DEMONSTRATES A GOOD ADHESION OF PAN CARBON FIBERS (RIGHT).	64

FIGURE 50: VOLUME RESISTIVITY OF HYBRIDS COMPOSITE CONTAINING 21%WT. OF A BLEND CONTAINING VARIOUS AMOUNTS OF STAINLESS STEEL AND CARBON FIBERS. POLYMERIC MATRIX USED IS PA6.....	67
FIGURE 51: PICTURE OF A BURNT HYBRID SAMPLE OBTAINED BY OPTICAL MICROSCOPY. SF ARE EXTREMELY FLEXIBLE (I.E. WAVY SHAPE) WHEN COMPARED TO CARBON FIBERS (I.E. STRAIGHT LINE).....	68
FIGURE 52: EVOLUTION OF YIELD STRENGTH OF HYBRIDS COMPOSITE CONTAINING 21%WT. OF A BLEND CONTAINING VARIOUS AMOUNTS OF STAINLESS STEEL AND CARBON FIBERS. POLYMERIC MATRIX USED IS PA6.....	69
FIGURE 53: FIBER LENGTHS COMPARISON BETWEEN SAMPLES CONTAINING 10%WT CARBON FIBERS IN HYBRID AND COMPOSITE.....	70
FIGURE 54: EVOLUTION OF FLEXURAL STRENGTH OF HYBRIDS COMPOSITE CONTAINING 21%WT. OF A BLEND CONTAINING VARIOUS AMOUNTS OF STAINLESS STEEL AND CARBON FIBERS. POLYMERIC MATRIX USED IS PA6.....	71
FIGURE 55: EVOLUTION OF ELASTIC MODULUS OF HYBRIDS COMPOSITE CONTAINING 21%WT. OF A BLEND CONTAINING VARIOUS AMOUNTS OF STAINLESS STEEL AND CARBON FIBERS. POLYMERIC MATRIX USED IS PA6.....	71
FIGURE 56: EVOLUTION OF IMPACT ENERGY OF HYBRIDS COMPOSITE CONTAINING 21%WT. OF A BLEND CONTAINING VARIOUS AMOUNTS OF STAINLESS STEEL AND CARBON FIBERS. POLYMERIC MATRIX USED IS PA6.....	72
FIGURE 57: INFLUENCE OF 2%CF PAN ON THE VOLUME RESISTIVITY OF A SAMPLE CONTAINING 10%CB. PA6 WAS USED AS POLYMERIC MATRIX.....	74
FIGURE 58: INFLUENCE OF 2%CF PAN ON THE YIELD STRENGTH OF A SAMPLE CONTAINING 10%CB. PA6 WAS USED AS POLYMERIC MATRIX.....	75
FIGURE 59: INFLUENCE OF 2%CF PAN ON THE FLEXURAL STRENGTH OF A SAMPLE CONTAINING 10%CB. PA6 WAS USED AS POLYMERIC MATRIX.....	75
FIGURE 60: INFLUENCE OF 2%CF PAN ON THE ELASTIC MODULUS OF A SAMPLE CONTAINING 10%CB. PA6 WAS USED AS POLYMERIC MATRIX.....	76
FIGURE 61: MELT FLOW INDEX OF SAMPLES CONTAINING 10% CB IN PA6, 2%WT. IN PA6 AND A MIX OF 10%WT. CB AND 2%WT. CF FIBERS.....	76
FIGURE 62: INFLUENCE OF 2%CF PAN ON THE IMPACT RESISTANCE OF A SAMPLE CONTAINING 10%CB. PA6 WAS USED AS POLYMERIC MATRIX.....	77

List of tables

TABLE 1: GLOBAL MARKET FOR CARBON BLACK (CY 2013). CB IS MAINLY USED IN TIRE APPLICATION AS REINFORCING AGENT. [8]	9
TABLE 2: COMMON METALLIC FILLERS AND RELATED ELECTRICAL PROPERTIES. Σ : ELECTRICAL CONDUCTIVITY RELATIVE TO COPPER, μ : RELATIVE MAGNETIC PERMEABILITY. ATTENUATION OCCURS BY THREE MECHANISMS: FIRSTLY, THE ABSORPTION RELATED TO THE PRODUCT $\Sigma \times \mu$. THEN THE REFLECTION RELATED TO THE RATIO Σ / μ . NICKEL AND STAINLESS STEEL ARE EXCELLENT FOR ABSORPTION WHEREAS SILVER AND COPPER FOR REFLECTION. [14]	12
TABLE 3 : TYPICAL VALUE FOR H_0 IN FIBER REINFORCED COMPOSITE.[25]	27
TABLE 4 : SUMMARY OF FILLERS USED IN THIS WORK AND MAIN PROPERTIES.....	32
TABLE 5 : MATRIX USED IN THIS PROJECT AND RELATED PROPERTIES.....	32
TABLE 6 : EFFECT OF PROCESS PARAMETERS ON FIBER LENGTH.....	43
TABLE 7: TSE COMPOUNDING OPTIMIZED SETTINGS	48
TABLE 8: VALUES ESTIMATED AND FROM DATASHEET USED IN RoM EQUATION	57
TABLE 9 : COMPOSITION OF EACH BLEND IN %WT. AND %VOL.....	66

List of abbreviations

CF	Carbon fiber
SF	Stainless steel fiber
CB	Carbon black
PAN	Polyacrylonitrile (precursors used for CF manufacturing)
PITCH	Oil – Petroleum (precursor used for CF manufacturing)
RoM	Rule of mixtures
RoHM	Rule of hybrid mixtures
TSE	Twin screw extruder
L_c	Critical fiber length
SE_t	Total shielding efficiency
EMI	Electromagnetic interference

1. General

1.1. Motivation

Polymers, particularly plastics, are generally electrical insulative materials with electrical resistivity generally above $10E+12 \Omega\text{cm}$ (Ohm.cm). They are extensively used in variety of applications thanks to their ease of shaping, low density, corrosion resistance and great flexibility in usage.[1]

Since the 1950's lots of investigations have been performed to bring electrical conductivity to polymers. Common way is to mix the polymer with conductive fillers such as carbon black, metallic particle, fiber, nanoparticle or metallic coated fibers. These compounds are generally referred as electrically conductive composite.[2]

Electrically conductive composites exhibit resistivity between metallic conductor ($1\Omega\text{.cm}$) and plastics insulator ($10E+12\Omega\text{cm}^{-1}$). They are increasingly used in electro static dissipation (ESD) application as substitutes to metals for weight and cost reduction. ESD can destroy sensitive electronic components or magnetic media, and even initiate fires or explosions.

Important examples are floor heating elements, electronic and electric equipment (cable, connectors, etc.), electromagnetic interference (EMI) shielding, sensing components and also in equipment requiring dissipation of static electricity as for instance in automotive part (fuel filler pipe and fuel lines, battery case, etc.) and ATEX (Atmosphere Explosive) environment. [2]

Cabot Corporation supplies a wide range of electrically conductive composite under the trademark CABELEC®. For decades, these compounds have successfully been used in application such as automotive fuel systems, electronic and electrical packaging and equipment. These conductive composite are essentially based on carbon blacks based filler. [3]

Carbon blacks are relatively low-cost fillers and are often used as pigment in plastics. Besides providing electrical conductivity, they can also be used as lasting protection against UV light. The main drawbacks, though, are that carbon black offers limited improvements in mechanical properties, often presents severe sloughing and significantly increase the polymer viscosity.
[3]

Nowadays there are high end applications that require conductive compounds with higher stiffness and/or toughness but such products are currently not available in Cabot portfolios. This increasing demand in high performance conductive compounds has driven Cabot to invest massively in the development of new products to meet performance requirements.

1.2. Project objectives

Within this framework, this master thesis aims to bring a thorough understanding of alternative solutions to carbon black as electrically conductive fillers for plastics.

The first step toward achieving this is to perform a comprehensive literature review of available conductive fillers and to identify potential substitute to carbon black.

The second step is to develop formulations based on these fillers in polyamide 6 (PA6) and polybutylene terephthalate (PBT) as polymer matrix. This is done to evaluate matrix effects on compound properties. Formulations have then to be incorporate into a viable manufacturing process available at Cabot laboratories in Pepinster.

Afterwards, these compound are characterized in terms of mechanical (tensile, impact and flexural), rheological (melt flow index) and electrical (volume resistivity) properties. These are important properties for industrial applications and allow pinpointing weaknesses and benefits of each filler.

Those results are then used to select fillers usable in hybrid (i.e. containing at least two different filler) composite and to evaluate possible synergistic effects between fillers.

Further microscopy (electronic and optical) studies are then performed to better understand how fillers and their dispersion state affect composite properties.

The last part of this work is dedicated to improvements and possible perspectives.

2. Theoretical background

This general introduction highlights composites application and advantages towards other “classical” materials. To derive the maximum possible benefit from composites, it is essential to understand the fundamental factors that dictate their properties. This chapter sets out a review of these factors.

2.1. Electrical properties of conductive composites

This chapter is divided into two sections where composite electrical properties basics are laid down.

In the first part, percolation phenomenon and its impact toward conductivity is discussed. Subsequently, the second part describes electron conduction mechanisms within the matrix.

- **Percolation phenomenon**

An important feature in composites is the percolation phenomenon which corresponds to a sharp decrease in electrical resistivity. This generally occurs above a critical fraction of filler (percolation threshold, φ_c).

According to statistical percolation theory, the conductivity (σ) is expected to follow a power law dependence of the form

$$\sigma = \sigma_c (\varphi - \varphi_c)^t$$

Equation 1

Where σ_c , φ and φ_c are respectively the conductivity at percolation, the volume fraction of filler above percolation and the volume fraction of filler at percolation. "t" is a critical exponent related to the dimensionality of the conductive network. It is around 1.33 in two and 2 in three dimensions.[3]

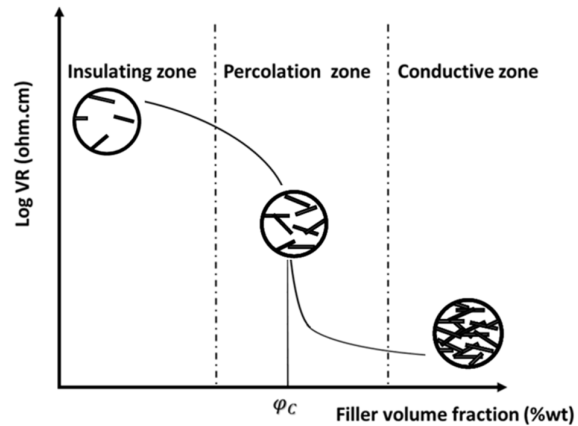


Figure 1 : Percolation phenomena scheme. Adapted from [1]

Beyond the percolation threshold (φ_c), a continuous conductive network of fillers is formed which allows the current to flow through the material and a drop in resistivity is observed (**Figure 1**). The resistivity then settles down and gets close to the conductive filler material [4]. Usually, it is preferred to have percolation threshold as low as possible for cost consideration and ease of processing. [2]

- **Electrical conduction mechanisms**

Electron conduction in composite has been extensively studied to explain the percolation phenomenon and several mechanisms were suggested. Among these tunneling of electron and conduction path theory are the most used [5][6]. Such theories are important in the design and selection of conductive fillers. Hereby we will briefly discuss basic concepts and focus on practical implications of such theories.

In conduction path theory, physical contact of conductive fillers leads to formation of continuous conductive chains within the insulating polymeric matrix. This allows electrons to flow through the material when electrical field is applied.

The main difference between conduction theory and tunneling theory (a special case of internal field emission), is that in tunneling quantum effects are considered which gives lower percolation threshold than predicted in the conduction theory. It is assumed that electron wave function is not confined within a barrier potential and is able to slightly extend beyond to penetrate the barrier of neighbor filler. [2]

Tunneling theory introduces the concept of "effective contact". It is assumed that when the insulating gaps between fillers particles reach a given distance (i.e. few nanometers) a high field strength is experienced between the two conducting area. This field can bring enough energy to an electron to jump across the gap and bring additional conduction. [2]

These lead to the concept of "critical concentration", the concentration at which the conductive fillers are close enough each other to reach percolation. Many statistical studies have been performed to evaluate this threshold but are often not accurate due to the complex combination of many factors to consider. However, it is worthwhile to pinpoint their qualitative implications. It is shown that geometrical aspects such as distribution, shape, particle size, and porosity are crucial factors impacting percolation threshold.

Lower particle sizes have statistically more probability to form conductive paths per unit volume thanks to their higher surface area. Moreover, they tend to sinter resulting in aggregates with smaller gaps and easier tunneling of electron. Another important parameter is the filler aspect ratio. This parameter is related to the filler shape and is defined as equal to the ratio between length and diameter of the filler. [2]

Particles with high aspect ratio ease the formation of conductive networks and lower the percolation threshold (**Figure 2**).

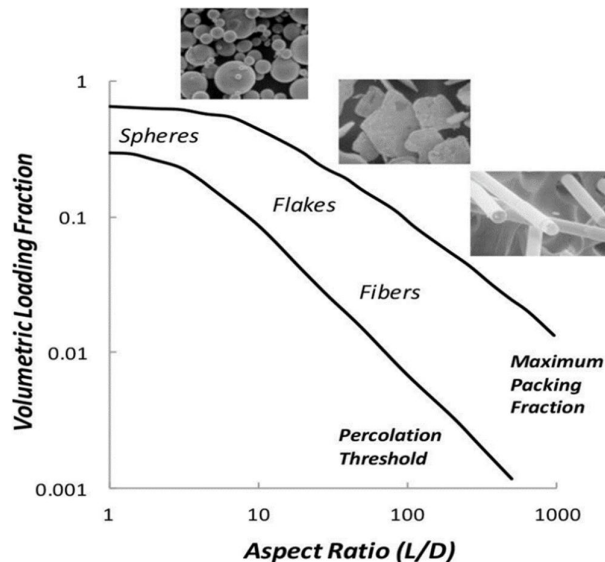


Figure 2 : Influence of aspect ratio on percolation threshold [7]

Besides filler properties, polymeric matrix also plays a critical role in composites electrical properties. Generally, matrix dictates shearing forces experienced by the fillers and also contribute to their selective localization. For instance, it is shown that parameters such as high polymer crystallinity lower the percolation threshold in semi-crystalline polymer (i.e. selective localization of fillers in amorphous region) whereas high polymer viscosity tends to raise it (i.e. high shearing and lower filler structure or aspect ratio). To a lesser extent, lower polarity of the polymer may also lower the critical fraction value.[2]

2.2. Material selection

As explained previously, we know that filler features (i.e. nature and shape) play major roles in composite properties.

Annex A-1 summarizes popular fillers and related characteristics and applications. Hereby, we focus on the materials selected (i.e. stainless steel fiber and carbon short fibers) as substitute for carbon black.

After a brief discussion on carbon black generalities, we will discuss benefits of using short fibers among other aspect ratio fillers (e.g. nanoparticles, spheres, etc.).

In third and fourth part, reasons that make stainless steel fibers and carbon fibers promising alternatives are presented.

- **Carbon black (CB)**

Carbon black is extensively used as reinforcing agent in the rubber industry providing enhancement in dimensional stability or in plastics as a pigment or UV stabilizer.

Owing its low electrical resistivity (ranging from 1 to 10^{-4} Ohm.cm), carbon black is also commonly used as conductive filler. **Table 1** summarizes main applications of CB in 2013 and related volumes.

Application/market	Quantity (ktons)	Main use
Total global carbon black consumption	11,360	
Rubber for tire applications	8,320	Reinforcing agent
Rubber for non-tire applications	2,240	Reinforcing agent
Plastics	350	Pigment, UV stabilizer
Plastics, rubber	105	Conductive additive
Surface coatings	190	Pigment
Ink	150	Pigment
Others	5	

Table 1: Global market for carbon black (CY 2013). CB is mainly used in tire application as reinforcing agent. [8]

Carbon black consists of carbon atom covalently bonded together in an amorphous form similar to disordered graphite. This amorphous form is referred as the "primary particle". It generally presents a spherical shape with nanoscale range size (**Figure 3**).

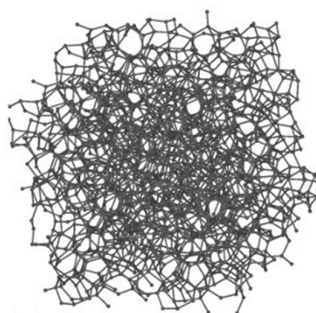


Figure 3: Carbon black primary particle consisting of carbon covalently bonded in an amorphous form. The primary particle usually presents a spherical shape and is around 50nm.[9]

Currently, 90% of the actual carbon black productions use the furnace process. Furnace process principle consist of thermally decompose a hydrocarbon oil to produce carbon black primary particles. This process allows producing primary particle ranging between 10 and 100 nm.

Several "primary particle" can fuse together to give aggregates with size up to 500 nm. Aggregates can be seen as a bunch of grapes where a single raisin corresponds to a primary particle. Aggregates can further weakly bond to other aggregates by Van der Waals (VDW) interactions resulting in agglomerates generally larger than 1 μm (Figure 4). Both primary particles size and aggregates dramatically depend on the manufacturing process.

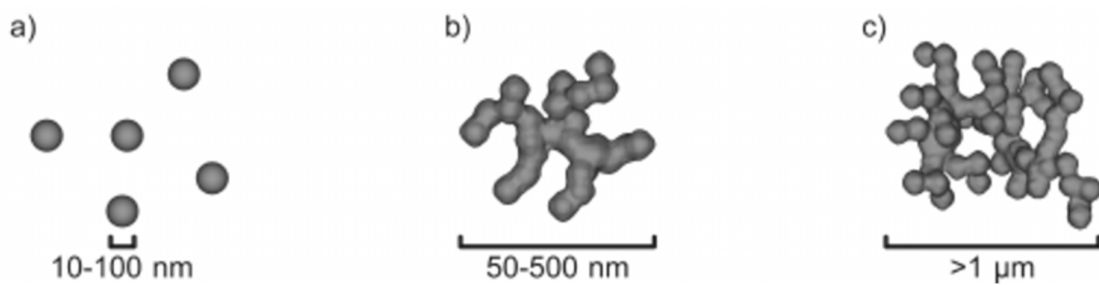


Figure 4 : Formation of agglomerate a) Primary particle made of carbon atom covalently bond, b) aggregate consisting of fused primary particle, c) Aggregate weakly bond together by VDW interaction to form agglomerate. [10]

- **Short fibers**

As indicated previously, short fibers (i.e. having length lower than 10 mm) reinforcements were selected for this work owing their unique combination of benefits among all investigated fillers aspect ratio.

Very small particles such as nanofillers (e.g. carbon nanotubes, graphene, etc.) provide exceptional conductivity and enhancement in mechanical properties. Nevertheless, resulting composites usually exhibit extremely high viscosity and therefore loss of processability (e.g. lower output and consequently lower productivity). Furthermore, owing their very small size they are difficult to disperse and tend to agglomerate to form large particles which are deleterious to some properties (e.g. toughness). They are currently difficult to produce on a large scale and expensive (e.g. approximately 500 €/kg for nanotubes) which make them cost non-competitive, even at very low filler content. To complicate matters further, they also present potential harmful effects. [11][12]

On the other hand, owing their relatively large size and high aspect ratio, fibers can dramatically improve properties in polymers (e.g. electrical conductivity, stiffness, strength, etc.) and do not suffer from nanofillers drawbacks (i.e. processability, harmful effects).

Lastly, although they are usually more expensive than classical fillers such as carbon black, the potential improvement in properties (mechanical and electrical) and low required loading enable them to be cost-competitive.

- **Stainless steel fiber**

Besides providing excellent conductivity (10^{-8} - 10^{-7} Ohm.cm), metal filled polymers are particularly interesting for electromagnetic interference (EMI) shielding application and are increasingly used as metal substitute for weight and cost reduction in electronic devices. They exhibit electrical characteristics closed to metals while mechanical and processing methods are typical for plastics. EMI is the disturbance of an electronic device when it is in the environs of an electromagnetic field (EM field) caused by another electronic device. EMI is of particular concern since it may cause dysfunctions in many electrical apparatus. [13]

Common metallic fillers (generally in form of flakes or fibers) are stainless steel, silver, copper, aluminum and nickel (**Table 2**).

Material	σ	μ	$\sigma \times \mu$	σ / μ
Silver	1.05	1	1.05	1.05
Copper	1	1	1	1
Gold	0.7	1	0.7	0.7
Aluminum	0.61	1	0.61	0.61
Nickel	0.2	100	20	2E-3
Stainless steel	0.02	500	10	4E-5

Table 2: Common metallic fillers and related electrical properties. σ : electrical conductivity relative to copper, μ : relative magnetic permeability. Attenuation occurs by three mechanisms: Firstly, the absorption related to the product $\sigma \times \mu$. Then the reflection related to the ratio σ / μ . Nickel and stainless steel are excellent for absorption whereas silver and copper for reflection. [14]

Total shielding efficiency (SE_T) is used to describe quantitatively shielding properties and is expressed in **Equation 2**.

$$SE_r = 10 \log \left(\frac{P_{in}}{P_{out}} \right) = SE_A + SE_R + SE_l \quad \text{Equation 2}$$

Where P_{in}/P_{out} represents the ratio between the incident signal and transmitted signal through a material. SE_R is reflection shielding efficiency and is directly related to the ratio σ / μ .

Owing their high conductivity and low magnetic permeability, silver and copper are excellent for reflection. On the other hand, absorption (SE_A) is proportional to the product $\sigma \times \mu$ which make stainless steel and nickel better due to their high magnetic permeability. SE_l is a correction term related to the reflecting waves inside the shielding barrier (multireflections). [14]

Shielding efficiency depends on the frequencies of the incident waves. Low frequencies waves are well blocked by reflecting materials (e.g. silver, copper) whereas higher frequencies usually require absorbing materials. [14]

Since the demand for apparatus operating at higher frequencies (e.g. smartphones) is increasing, nickel and stainless steel filled polymer consumption are expected to dramatically grow. With that in mind and owing its higher corrosion resistance and relatively low price toward nickel, stainless steel was chosen for this project. [13][14]

- Carbon fiber

For decade carbon fibers have been successfully used in niche sectors such as aerospace, civil engineering, military or sport industry but their high price made them prohibitive for civil usages.

Many researches have been performed on carbon fibers manufacturing to reduce costs. Within this framework, recent progresses are supposed to dramatically lower their price.[15][16]

Since concerns about CO₂ emissions are growing, carbon fibers uses are expected to grow, especially in the transport and energy industry (e.g. wind industry and cars) where light weighting and performance are key points (Figure 5).

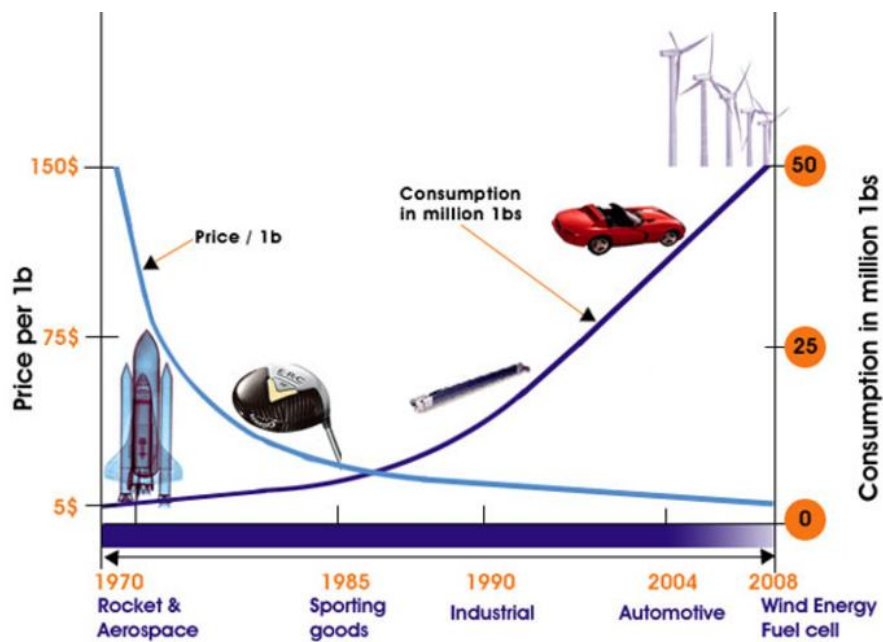


Figure 5 : Trends and forecast in carbon fiber shipment.[8]

Carbon fibers are of considerable interest because they possess a unique performance to weight ratio. They offer high thermal and electrical conductivity, high stiffness, high tensile strength, high chemical and temperature resistance, low thermal expansion and possess low density.

This unique set of properties allows them to be used, often incorporated into a polymer matrix, as replacement for metallic structural parts.

Carbon fibers, like graphite, are set up with pile of graphene sheets, the main difference being the arrangement of these sheets (**Figure 6**).

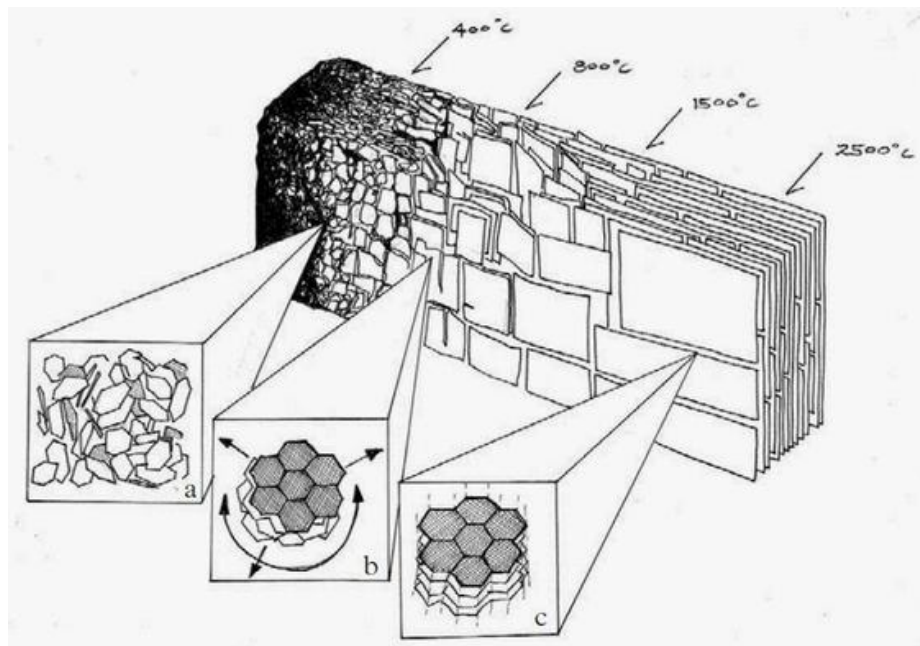


Figure 6 : Carbon fiber illustration representing sheets interlocking at different temperature. It shows transformation of carbon structure with temperature: (a) amorphous (non-crystalline) at 400 °C, (b) turbostratic crystallites at 800 °C, and (c) graphene sheet structure (graphite) dominant above 1100 °C. [17]

Depending upon the precursors and conditions, those sheets can be oriented either randomly (i.e. turbostratic), parallel to the fiber axis (i.e. graphitic) or between.[18]

Nowadays, 90% of the current carbon fiber production use polyacrylonitrile (PAN) as precursors, while remaining 10% are shared between PITCH and to a lesser extent Rayon (cellulose).

PAN carbon fiber (turbostratic) displays electrical resistivity ranging from 10^{-3} to 10^{-5} Ohm.cm. They are generally strong and though. On the other hand, PITCH (graphitic) carbon fiber is more conductive (10^{-4} to 10^{-6} Ohm.cm) than PAN carbon fiber and also more stiff (**Figure 7**).

In this work, both (PITCH and PAN) carbon fibers are investigated.

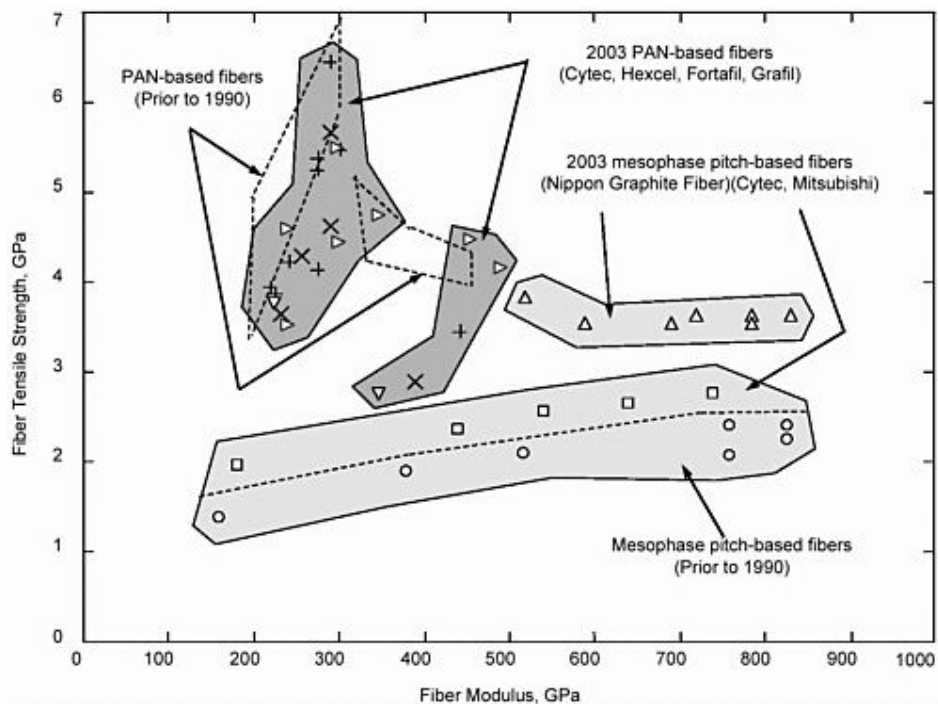


Figure 7 : Carbon fibers classification according to precursors used during the manufacturing. PAN fibers are usually stronger and less stiff whereas PITCH fibers are stiffer and less strong.[19]

Carbon fibers manufacturing involves 3 steps regardless the precursor used (i.e. stabilization, carbonization and graphitization). As an example, PAN carbon fibers manufacturing will be briefly described below.

During stabilization, precursor fibers are heated in air at about 300°C which allow cyano side group to be cyclized (**Figure 8**).

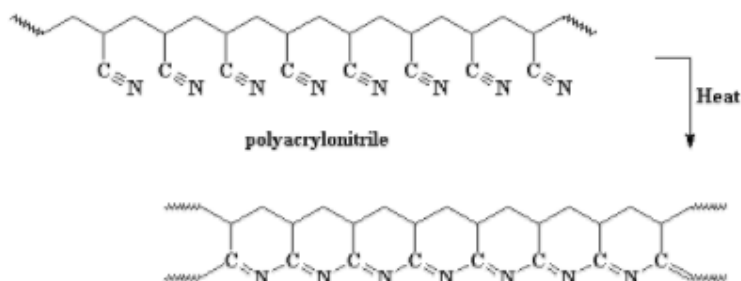


Figure 8 : Stabilization step in carbon fiber production process. The PAN fibers are heated at 300°C and their cyano side group react together to form stable cyclic ring.[20]

Afterwards, fibers are heat up to 700°C to eliminate hydrogens and form aromatic pyridine groups (**Figure 9**).

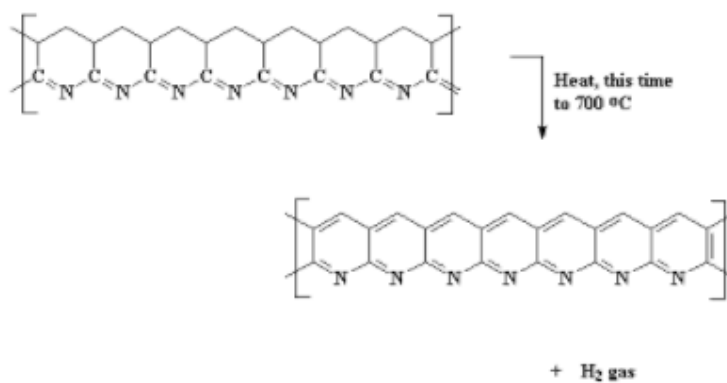


Figure 9 : Second step of stabilization step in carbon fiber production process. Fibers are heated to 700°C allowing elimination of H₂ and formation of aromatic pyridine which can further fused with other chains. [20]

Fibers are then carbonized. Carbonization consists of two steps: the first step involves moderate heating (i.e. 400 – 600°C) in an inert atmosphere.

This is done to remove residual non-carbon atoms and allow adjacent chains to fuse together (**Figure 10**).

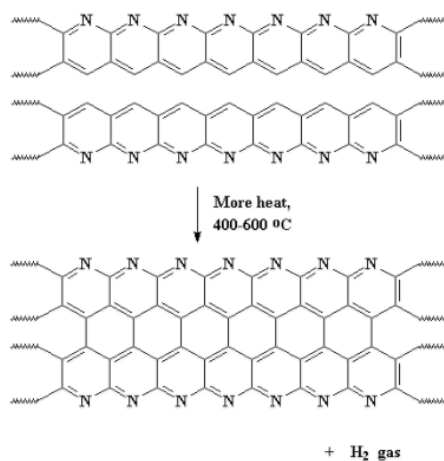


Figure 10 : Carbonization first step: Elimination of remaining impurities and fusion of adjacent chains. This is done by further heating of the previously obtained aromatic pyridine chains. [20]

The second step occurs at higher temperature, between 600°C and 1300°C. It allows the growth of “graphene like” sheets (**Figure 11**).

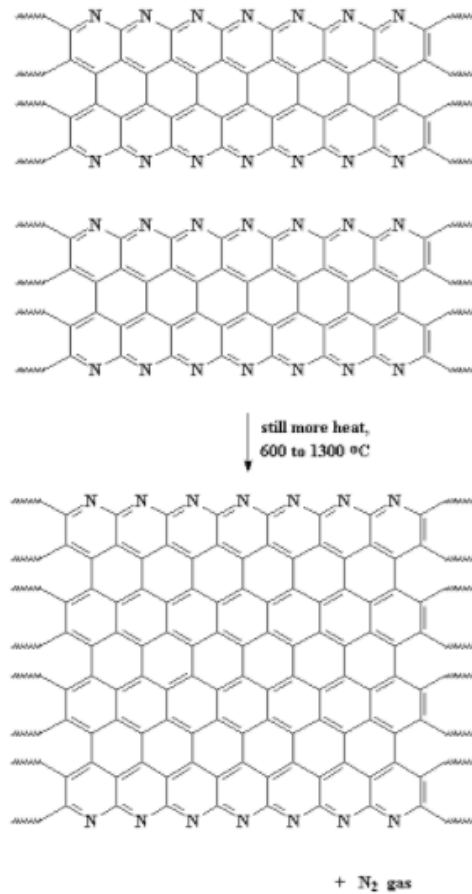


Figure 11 : Ribbons fused together to give larger ribbons. Each ribbon contain carbon in its hexagonal structure [20]

Carbonization leads to formation of turbostratic carbon (i.e. amorphous) presenting a regular hexagonal graphitic structure (**Figure 12**).

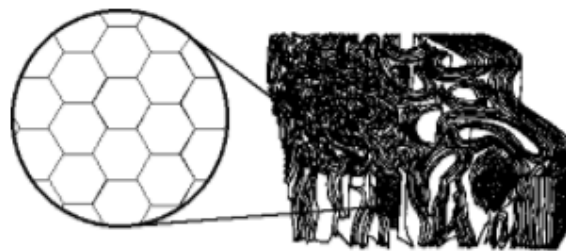


Figure 12 : Turbostratic carbon fibers: Carbon are highly ordered in the short range but not at higher range [20]

Graphitization is an optional step. It consists in prolonging heating treatments at high temperature (between 1300 and 3000°C) which make graphene sheets larger and increase ordering until eventually formation of pure graphite. This is the stacking of these sheets which is responsible for carbon fiber mechanical properties. [19]

2.3. Mechanics of short fiber reinforced polymers

In this work, besides electrical properties, considerable attention has been given to study the mechanical behavior of composites (i.e. strength, stiffness and toughness).

This chapter sets out basic fibers properties required for manufacturing good mechanical performance composites.

It is structured in three sections wherein basic aspects of these properties are discussed. First section is dedicated to the "critical fiber length" notion and its importance toward mechanical properties whereas second section deals with surface chemistry of fibers, especially surface treatments and sizing.

The last part is dedicated to a brief discussion on the rule of mixture for composite elastic properties prediction.

- **Critical fiber length (L_c)**

Continuous long fibers (few centimeters or more), although providing outstanding composite performance, are often inconvenient to use in many applications. This is because they usually require to be processed by techniques such as compression molding to avoid fiber degradation.

Comparing to injection and extrusion molding, such techniques are time consuming, expensive and lack of flexibility.

For years, engineers have figured out that composite almost as strong as those obtained by compression can be achieved by injection molding as long as the fibers exceed a critical length.

This critical length [21] was evaluated to be equal to:

$$L_c = \frac{\sigma_f d_f}{2\tau_m} \qquad \text{Equation 3}$$

L_c is the length at which the middle of the fiber reaches the ultimate tensile strength (σ_f) assuming a maximum shear strength (τ_m). d_f represents the diameter of the fiber. [21]

It has been established that to achieve effective enhancements, fibers have to be at least equal to the critical length L_c .

When a tension is applied to a composite, a shear stress occurs in the matrix that pulls from the fiber, uniformly along its axe (isostrain rule). As a consequence, the force on the fiber is maximum in the middle and minimum at the ends (**Figure 13**).

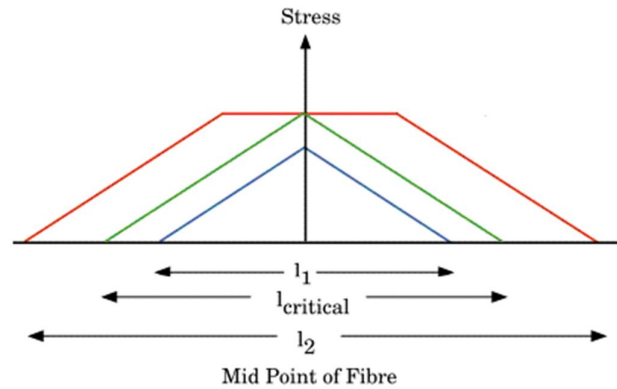


Figure 13 : Repartition of the load along fiber axis. Stress is maximal in the middle and minimum at the ends. When the fiber is shorter than the critical length, the applied strain is not totally transferred to the fiber and matrix may fracture before fibers (l_1). At the critical length, the load is effectively transfer. Consequently, fibers and matrix fail at the same stain and the composite is effectively reinforced (l_c). Beyond the critical length, the fibers will carry an growing fraction of the applied load (l_2).[21]

Now that theoretical basics are laid down, hereafter, critical lengths for each fiber are assessed using **Equation 3**.

PAN and PITCH carbon fibers have tensile strength of 4200 MPa and 3430 MPa respectively (see data sheets in **Annex A-2**). Assuming both shear strengths to be approximately equal to 50 MPa [22] and fiber diameters of 8 μm (PAN) and 10 μm (PITCH). Calculated critical lengths are 335 μm for PAN carbon fiber and 343 μm for PITCH carbon fiber.

No data on stainless steel – PA6 shear strength was found. Nevertheless, knowing that stainless steel usually exhibits poor adhesion toward polymeric matrix, one can assume that this value has to be extremely low. As a consequence, L_c for stainless steel should be extremely high and thus no reinforcements are expected. [23]

- **Surface treatments and sizing**

Previous chapter discussed the concept of fiber critical length (L_c). L_c was obtained using **Equation 3**.

$$L_c = \frac{\sigma_f d_f}{2\tau_m} \quad \text{Equation 3}$$

Besides L_c , **Equation 3** also reveals the importance of fiber adhesion which is reflected by maximum shear strength (τ_m) term.

Fiber-matrix adhesion plays a critical role in mechanical properties of composites. It allows effective load stress transfer from the matrix to fibers, and consequently allows fibers to efficiently carry the load. Furthermore, improved adhesion between fibers and matrix leads to better dispersion resulting in better composite performance.

Promoting fiber adhesion to polymeric matrices is a major challenge in composite manufacturing since untreated fibers are often inert toward polymeric matrix. In this context, several techniques were developed to enhance adhesion. These are generally classified within two groups.[23]

The first group concerns surface treatments modifications. Surface treatments consist in modifying the fiber surface by different means (e.g. electrochemical, chemical, thermal, discharge plasma etc.).

On the other hand, the second group don't directly modify fibers surface. Instead fibers experience a coating procedure called sizing application.

Sizing forms a polymeric layer (which is often epoxy based resins) around fibers which will acts as an interface between matrix and fibers.

Besides enhancing adhesion, sizing also protects fibers during processing.

Depending on the sizing formulation and its amount, final performances (electric, thermal and mechanical) of composites can largely vary.

- **Rule of mixture (RoM) for mechanical properties prediction in composites**

This section discusses the application of RoM for elastic properties (strength and stiffness) predictions.

RoM is an approximation method that estimates composites properties. This method assumes that composite properties are a volume weighted average of the phases (matrix and fillers) properties and that fiber adhesion toward matrix is optimal. [24] [25]

We observed in **section 2.3** (critical fiber length) that composite elastic properties were strongly correlated to fiber length. Moreover, it has also been demonstrated [24] that fibers orientation in the composite also plays a critical role (**Figure 14**) Unidirectional (UD) orientation will lead to higher tensile properties whereas isotropic materials tend to exhibit relatively lower performances.

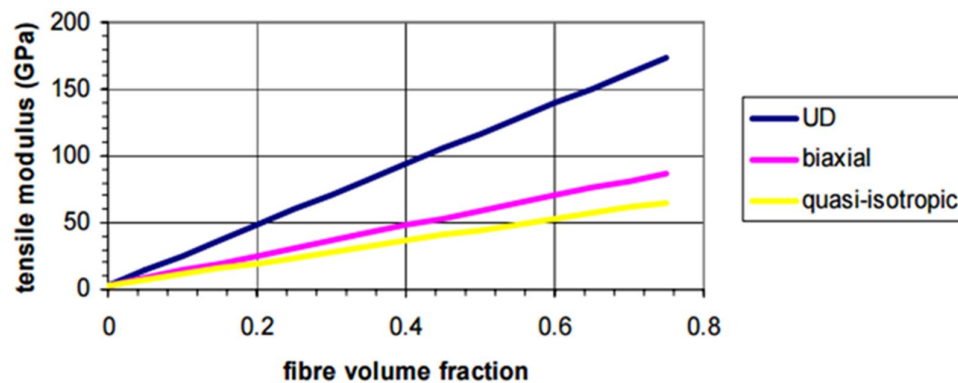


Figure 14: Effects of fiber orientation on tensile modulus of carbon fiber reinforced epoxy resins.[25]

As a consequence, RoM equation when applied to mechanical properties of short fiber reinforced composites usually contains the correction terms η_l (length) and η_0 (orientation) (**Equation 4**).

$$E_c = \eta_l \eta_0 E_f V_f + E_m (1 - V_f) \quad \text{Equation 4}$$

Where E_c , E_f and E_m represents an elastic properties (i.e. elastic modulus or tensile strength) of composite, filler and matrix respectively. V_f represents the volume fraction of filler. (note that $(1 - V_f)$ is simply the matrix volume fraction).

η_l is a length correction factor which tends to 1 for fiber length beyond the critical length (L_c) and 0 below L_c .

This is illustrated in **Figure 15** where the evolution of η_l is displayed as a function of fiber length in an epoxy resin filled with glass fibers.

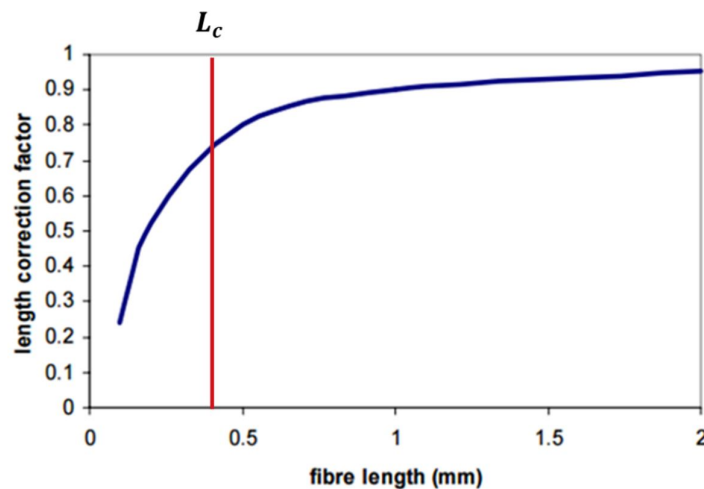


Figure 15: Length correction factor correlation with fiber length applied for glass fiber reinforced epoxy resin. Adapted from [25]

η_l can be calculated using the following formula:

$$\eta_l = 1 - \frac{2}{\beta L} \tanh\left(\frac{\beta L}{2}\right) \quad \text{Equation 5}$$

Where L is the fiber length and β a term that takes into account fiber adhesion, tensile properties of fibers, the distance between fibers and the fiber diameter.

According to literature [26], for short fibers (i.e. length lower than 1mm), the term $\frac{2}{\beta L} \tanh\left(\frac{\beta L}{2}\right)$ can be approximated as follows :

$$\frac{2}{\beta L} \tanh\left(\frac{\beta L}{2}\right) \approx \frac{L_c}{2L} \quad \text{Equation 6}$$

Where L_c is the fiber critical length. Hence, **Equation 4** can be rewritten:

$$E_c = \eta_0 E_f V_f \left(1 - \frac{L_c}{L}\right) + E_m (1 - V_f) \quad \text{Equation 7}$$

η_0 is a correction factor for non-unidirectional reinforcement. For perfectly aligned fibers, η_0 is equal to 1.

Table 3 below summarizes typical value for η_0 .

Fibers orientation	η_0
Unidirectional	1
Random (in plane)	0.375
Random (3D)	0.2

Table 3 : Typical value for η_0 in fiber reinforced composite.[25]

2.4. Fiber compounding

Previous chapters pinpoint importance of fiber length over mechanical (e.g. critical fiber length) and electric (e.g. aspect ratio) properties. It is known that severe fibers breakage usually occurs during compounding.

Main mechanisms of degradation are shear in the melt phase, or at the mold/barrel walls and fiber-fiber interactions.

Compounding of short fiber composites is generally achieved by internal mixers, single screw extruder, co-kneaders or twin screw extruders.

In this work, twin screw extrusion (TSE) was selected as compounding technique. Although TSE theoretically leads to higher fiber breakage when compared to other techniques, its flexibility allows minimizing this phenomenon (e.g. tuning of side feeder positions, screw speed, throughput, screw profile, etc.).

Moreover, this technique enables continuous production and higher productivity (since screw wear effects can be compensated by screw speed resulting in less down-time). Lastly, TSE is largely used in Cabot plants which eases potential scale-up.

TSE has basically four main parts. The first part is the feeding systems composed of one or more loss in weight gravimetric (LWG) feeders. They feed in a controlled manner the extruder via a hopper or a lateral stuffer with polymers, fillers, additives, etc. The extruder contains two co-rotating screws that mix and convey the materials through the exit die (i.e. third part). This die allows shaping of the materials as it leaves the extruders. Last part consists in downstream auxiliary equipment that cool, cut and collect final product (**Figure 16**).

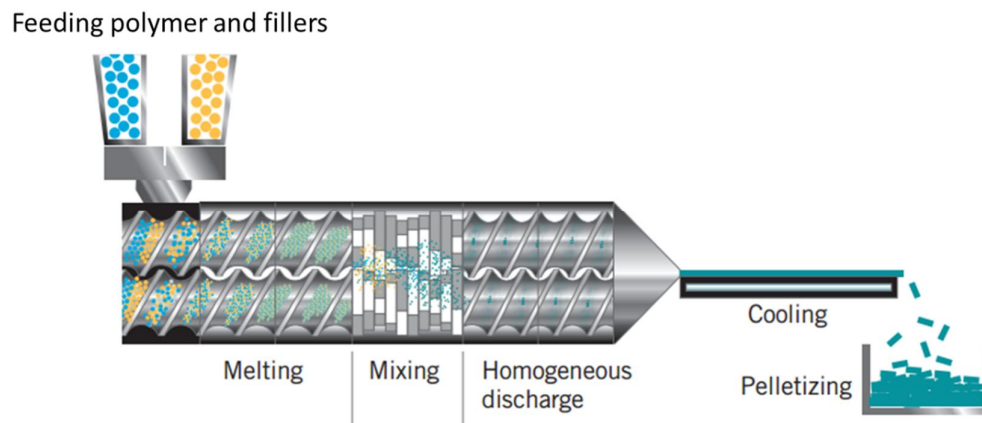


Figure 16: Twin screw extruder: schematic apparatus [27]

2.5. Hybridization

Composites containing more than one type of fillers are called hybrids. They usually exhibit unique features that can be tuned to meet various requirements.

In the case of composites, performance of hybrids may be evaluated by the rule of hybrid mixture (RoHM) equations. [27]

Interestingly, when using fillers presenting very different aspect ratios (e.g. fibers and carbon black) and intrinsic structure (e.g. metal and carbon), it is sometimes possible to observe deviations from RoHM. [40] These deviations are either due to enhancement (i.e. positive hybrid, synergistic effects) or degradation (i.e. negative hybrid effects) of composites properties. (Figure 17)

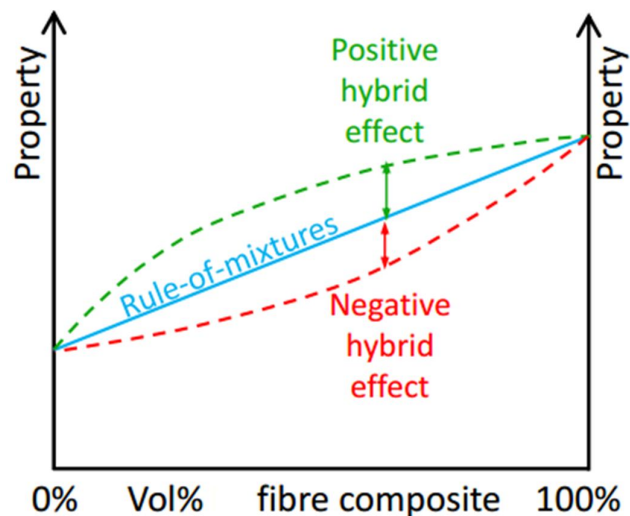


Figure 17: Hybrid composites usually follow a rule of mixture. Deviation from this rule may be observed when positive (synergistic) or negative hybrid effects occur. Adapted from [25]

In this work, two hybrids are investigated. The first hybrid is based on stainless steel and low-cost carbon fiber and is expected to provide conductive compounds exhibiting high shielding properties and enhanced mechanical properties when compared to simple stainless steel fibers based composite.

Furthermore, this hybrid should have better performance to weight - cost ratio since stainless steel fibers are more expensive (i.e. 65 €/kg vs 22 €/kg) and denser (i.e. 7.7 VS 0.5) than carbon fibers. The second hybrid is based on carbon black and carbon fibers and is expected to have a better balance between properties and cost when compared to regular carbon black or fiber composites.

3. Materials and methods

This chapter presents the experimental set-up applied in this research project. This is divided into, **section 3.1** about materials, and subsequently **section 3.2** which describes sample preparation. Lastly, **section 3.3** is devoted to sample characterization techniques.

3.1. Materials

Fillers and matrix used in this work are summarized in **Table 4 and 5** below.

Material	Brand	Properties	Length	Sizing	Cost	Manufacturer
Carbon black	VULCAN® XCMAX™22	Conductive filler	NA	NA	Low	Cabot
Carbon fiber PAN	DOWAKSA® AC4102	Conductive, high tensile strength	6mm	PA	Medium	DowAksa
Carbon fiber PITCH	GRANOC® XN-80C-06S	High conductivity, high elastic modulus	6mm	Epoxy	Very high	Nippon Graphite Fiber
Stainless steel fiber	Beki-shield® GR75/C16-E/4	EMI shielding, conductive	6mm	polyester	High	Bekaert

Table 4 : Summary of fillers used in this work and main properties

Matrix	Manufacturer	Brand
Polyamide 6	Dupont	Zytel® ST7301 NC010
Polybutylene terephthalate	BASF	Ultradur® B4500

Table 5 : Matrix used in this project and related properties.

3.2. Samples preparation

- **Twin-Screw compounding**

This project can be divided into two parts. In the first part, compounding settings were optimized to minimize fibers degradation. Afterwards, based on optimized settings, fillers and matrix effects on composites properties were evaluated.

All samples were dried one-night prior compounding. The TSE used was an APV MP30AC 40:1 with a screw diameter of 27mm and a barrel length of 40.5D. The screw profile has 30.5D conveying elements and 10D mixing elements. It was chosen to provide acceptable dispersion and moderate shearing. Detailed screws configuration is mentioned in **Annex A-3**.

A side feeder, positioned at 13.5D, was used for sensitive materials (i.e. carbon fibers) in order to limit their degradation (**Figure 18**). Other materials were fed into the main throat of the extruder using principal feeders (i.e. stainless steel fibers, carbon black and polymers).

Detailed compounding parameters and composition for each sample are mentioned in **Annex A-4**.

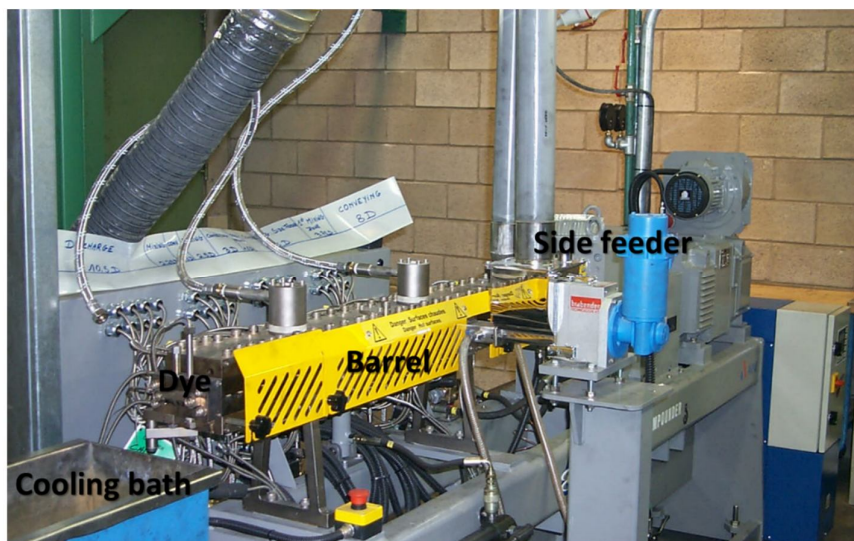


Figure 18: APV MP30AC 40:1 illustration of main parts (i.e. barrel, dye, cooling bath and side feeder)

The extruded strands were quenched into water at room temperature and then chopped into granules and stock into oven at 80°C to avoid moisture absorption.

- **Injection molding**

Injection molding is a common industrial process used to produce variety of plastic parts, from simple components to entire body panels of cars. Basically, this process involves to feed the desired material pellets into a barrel where pellets are melted, mixed and then injected into a mold cavity. In the cavity, materials are cooled and desired parts collected. (Figure 19)

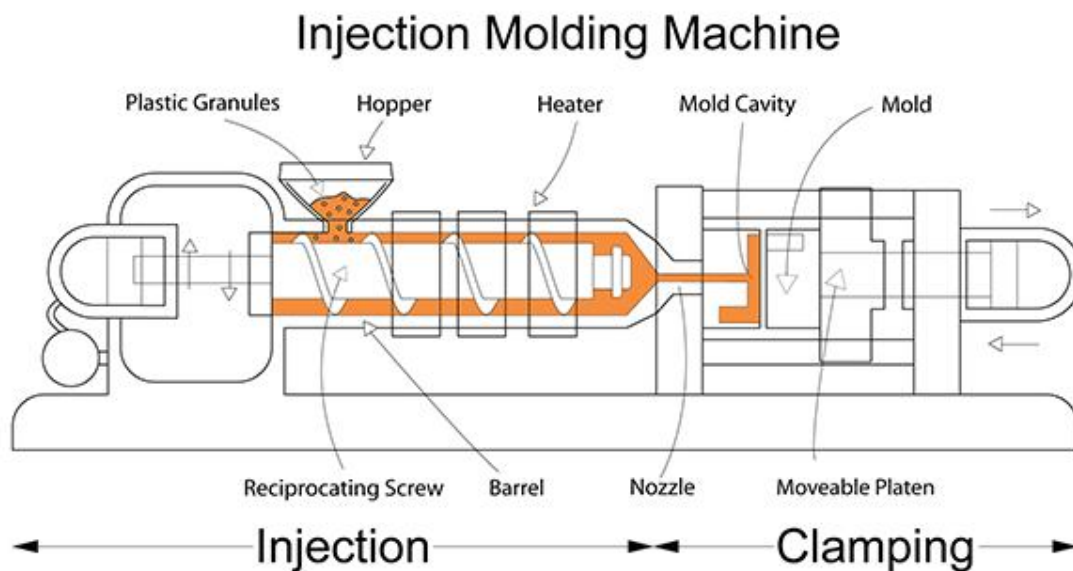


Figure 19: Injection molding machine schematic apparatus. Pellets are fed by a hopper into a heated barrel that mixes and injects melted materials into a mold. [28]

In this work, injection molding was used to prepare samples for electrical and mechanical characterization. All samples were injected using a single screw injection molding machine (Battenfeld BA500/200CD unilog 4000). The barrel and mold temperature were fixed at 240°C and 85°C respectively.

3.3. Characterization techniques

- **Fiber lengths**

Prior to length measurements, fibers have to be extracted from the polymeric matrix. It was done by carbonization at 900°C for 5 minutes under ambient conditions. Fibers were then collected and deposited on glass slides.

Image were acquired with a Leica DM LM optical microscope in transmission mode and recorded with a LEICA DFC295 camera (**Figure 20**).



Figure 20: Leica DMLM optical microscope and related Leica DFC295 camera

Straight fibers (i.e. carbon fibers) images are then proceed using Image J software. The 2D images are then converted into binary image and color thresholded automatically. Images are then automatically analyzed and average fiber lengths measured. (Figure 21)

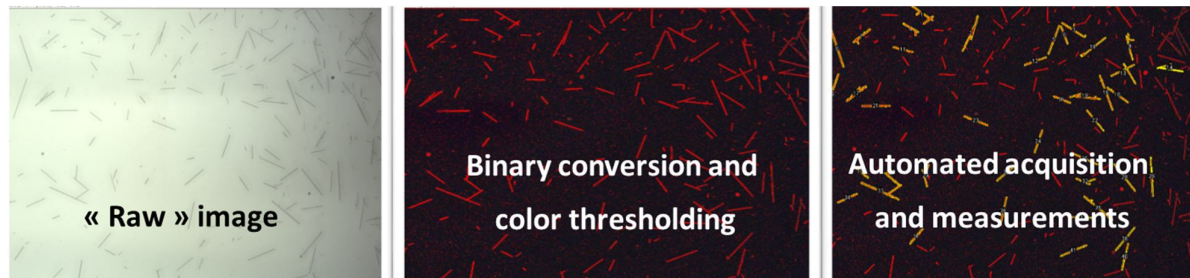


Figure 21: Image analysis process

Curved fibers (e.g. stainless steel fibers) are measured manually using image J software.

- **Volume resistivity**

The volume resistivity is obtained from the measurement of the resistance with which material opposes to a flow of electrical charges. This resistance is the ratio of the potential gradient (volts) parallel to the current direction against the intensity of the current (amperes) flowing in the material between the measurement electrodes. The principle of the measurement is described in ASTM D-4496 & D-257 and also in IEC93.

Volume resistivity measurements are performed on dried 4 x 50 x 80 mm plaque samples prepared by Injection molding press (Battenfeld BA500/200CD unilog 4000).

A homogenous coat of conductive silver paint is applied with a paintbrush on the two opposite sides of the injected plaque. Electrical resistance between the painted electrodes is then performed with a Keithley picoammeter.

The volume resistivity is then obtained applying the following formula:

$$VR = \frac{R * S}{d}$$

Where VR is the volume resistivity (ohm.cm); R is the average of the 3 resistance measurements (ohm); S is the perpendicular cross-section of the sample parallel to the measurement electrodes (= 2 cm²) and d is the distance between the electrodes (= 8 cm).

- **Tensile properties**

Tensile properties such as yield strength (σ_y) and elastic modulus (E) have been measured. These are useful information to evaluate strength and rigidity of a material.

Typically, those data are extracted/calculated from stress-strain curves (Figure 22).

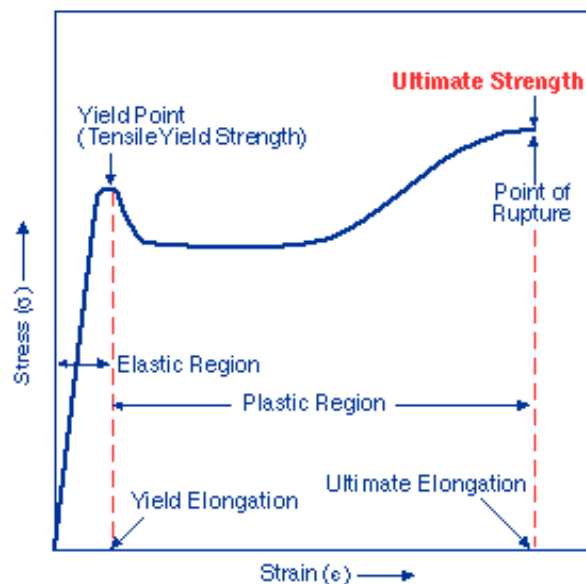


Figure 22: Stress - strain curves and related properties. [29]

Stress – strain curves are obtained using an extensometer. An extensometer is a device that measures length variation of an object when it is stretched or compressed.

In this project, an INSTRON 4411 tensile tester, 5kN cell, equipped with a set of mechanical self-blocking grips for rigid specimen, was used. Data are collected on the software Instron Series IX. Tensile dumbbells are obtained by injection molding (according to ISO 527-2/1B for rigid materials).

- **Flexural strength**

Flexural strength (σ) is defined as the maximum stress before yielding in a three point bending flexural test.

During a three point bending flexural test, the sample is placed on two supporting pins a set distance apart and a third loading pin is lowered from above at a constant rate until sample failure (**Figure 23**).

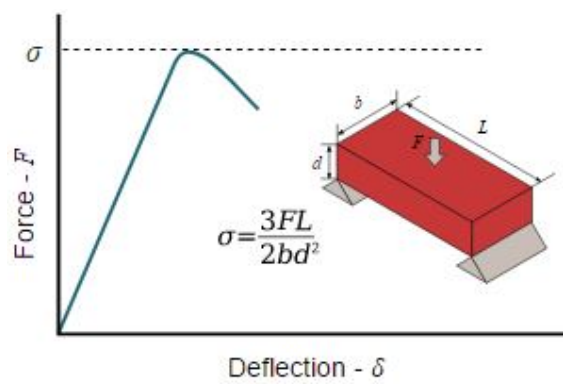


Figure 23: Three point bending flexural test. [30]

Measurements were performed on injected 80x10x4 mm³ bar specimen using an INSTRON 4411 equipped with 10 mm diameter upper anvil and 4 mm diameter lower anvils. Data are collected on the software Instron Series IX.

- **Notched impact resistance**

Impact resistance is useful information to evaluate the toughness of a material. It corresponds to the amount of energy absorbed by a material during an impact test. Notched Izod impact test according to ISO 180A is widely used in the plastics industry and has been used in this study. The test is performed by using a pendulum of known mass and dimension that is dropped from a known height to impact a notched specimen bar. The difference between the hammer height before and after the fracture allows calculating the transferred energy.

The IZOD impact strength is given by the energy extracted from the pendulum-type hammer in breaking the standard notched test bar, in a single pendulum swing. This energy is reported to the un-notched cross section of the sample.

It is given by the formula:

$$IZ = \left(\frac{E}{S}\right) * 1000$$

And

$$S = X * Y(k)$$

Where: IZ is the IZOD impact strength in kJ/m². E is the energy absorbed by the test bar breaking in J. X is the measured width of the test bar close to the notch place, in mm. Y(k) is the depth of the material remaining in the bar under the notch, in mm (**Figure 24**).

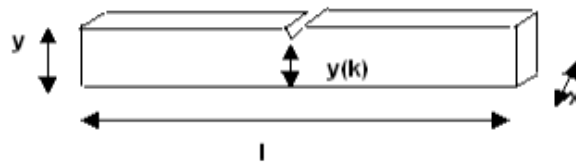


Figure 24: Bars and notches size.

Measurements were performed on injected 80x10x4 mm³ bar specimen using a pendulum-type hammer (Zwick 5113.300). A notching device (CEAST 6530) was used to realize Type A notch as described in ISO180-2000.

- **Scanning Electron Microscopy (SEM)**

In this work, SEM was used to visualize fibers surface and determine the quality of fiber adhesion to the matrix after compounding.

This technique is based on the detection of secondary electrons arising from an object after impact of a beam of primary accelerated electrons that scans its surface. [31]

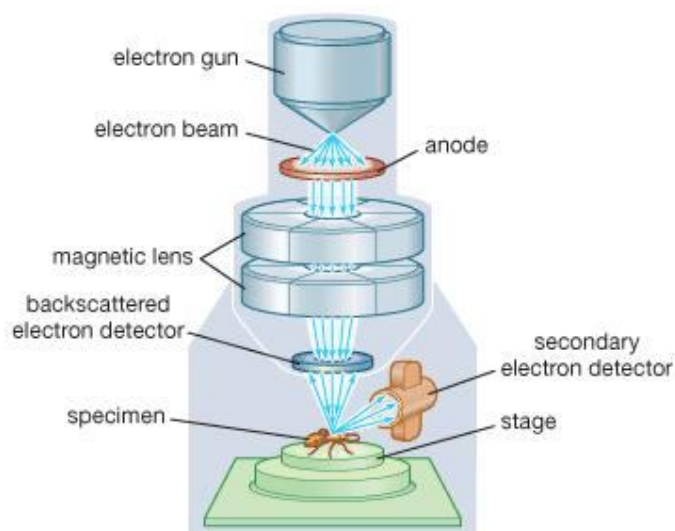


Figure 25: Scanning Electron Microscope principle illustration. [32]

The scanning electron microscope used in this work was an ESEM: PHILIPS ESEM XL30 FEG.

The accelerating voltage was of 7.5kV.

4. Results and discussions

This chapter summarizes the results obtained during this project. To facilitate reading, it is divided into three sections. (Figure 26)

Purchased carbon fibers are generally damaged after compounding due to the shearing forces experienced. In first section, the effects of main TSE parameters (i.e. screw speed, throughput, temperature and fiber weight percentage) on fiber lengths are investigated and optimized to minimize shearing effects and produce composite exhibiting high performances.

Subsequently, based on optimized settings, the effects of selected fillers toward electrical and mechanical properties of composites are assessed. In addition, two polymeric matrices (PA6 and PBT) were used to evaluate matrix effects on composite performance.

In the third part, hybrids (i.e. containing at least two fillers) compounds are evaluated and compared to single fillers system.

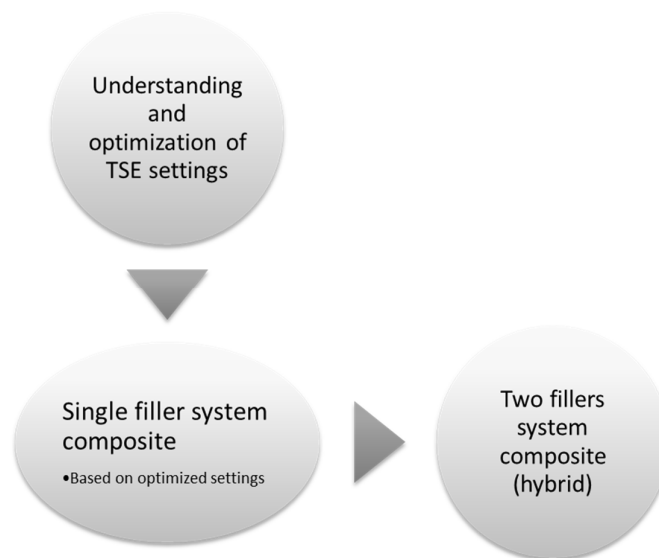


Figure 26: Results structure plan

4.1. Twin screw extrusion (TSE) compounding optimization

In this section, the effects of TSE parameters (i.e. screw speed, throughput, temperature and filler weight percentage) on fiber lengths are investigated. Carbon fibers were selected for this campaign. This is because they are more brittle than stainless steel fibers and consequently should represent the “worst case” scenario.

Table 6 below summarized obtained results and experimental conditions.

Tested parameter	Output rate			Screw speed			Weight percentage			Temperature		
	% wt.	Screw speed (rpm)	Throughput (Kg/h)	Temperature (°C)	Count	Average fiber length (μm)	95% confidence interval (μm)					
% wt.	10	10	10	10	10	10	10	30	40	10	10	10
Screw speed (rpm)	300	300	300	100	300	500	300	300	300	100	100	100
Throughput (Kg/h)	5	10	15	10	10	10	10	10	10	10	10	10
Temperature (°C)	263	269	265	273	269	276	269	278	277	239	273	307
Count	120	96	134	54	60	75	94	110	80	75	54	115
Average fiber length (μm)	217	284	272	346	322	270	284	251	248	270	330	346
95% confidence interval (μm)	15	15	17	29	15	25	15	17	18	22	29	34

Table 6 : Effect of process parameters on fiber length

For each tested settings, it was observed that fiber lengths were reduced to approximately 5% of their initial lengths (6 mm). Those results are consistent with those reported in literature [33] and illustrate the high shearing that fibers experienced during TSE compounding.

- **Influence of screw speed on residual length of fibers**

As displayed in **Figure 27**, higher screw speed leads to lower fiber length for all cases.

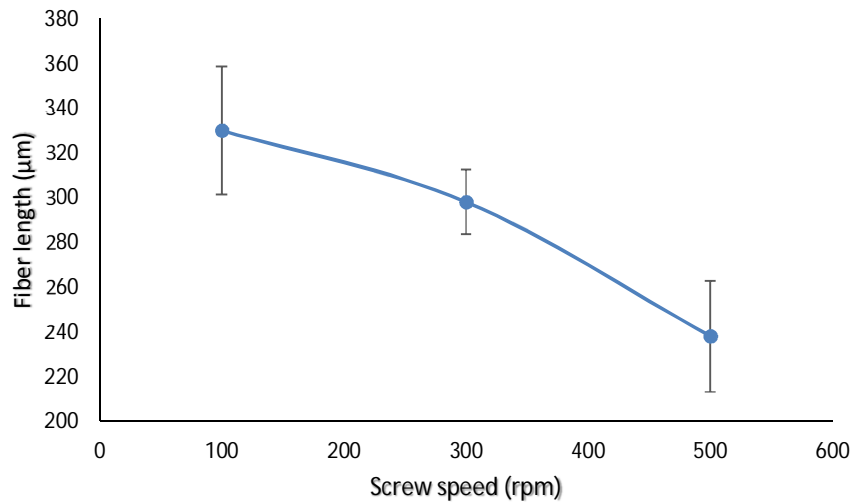


Figure 27: Influence of screw speed on residual length of carbon fibers

The largest increase in fiber degradation occurs between 300 and 500 rpm whereas results for 100 and 300 rpm are quite closed.

This can be explained by the shear thinning phenomenon illustrated in Figure 28.

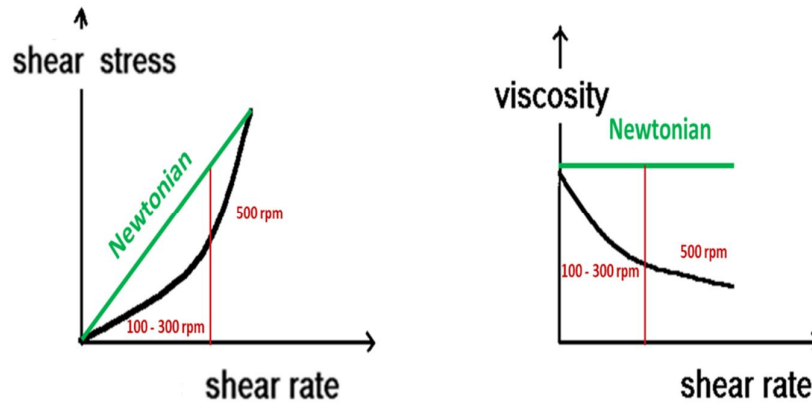


Figure 28: Shear thinning phenomenon illustration [34]

Shear thinning appears when the applied shear stress induced by TSE exceeds a critical value and results in a drop of the apparent viscosity.

Lower viscosity lowers the shear stress. As a result, fibers degradation appears to be less than proportional to the screw speed in this region.

At extreme shear rate (i.e. 500rpm), the melt behaves again like a Newtonian fluid [34]. The viscosity settles down, resulting in increased shear stress and subsequently higher fiber degradation.

- **Influence of output rate on residual length of fibers**

The influence of output rate on residual fibers length is displayed on **Figure 29**.

Fibers degradation dramatically decreases between 5 and 10 kg/h and settles down between 10 and 15kg/h.

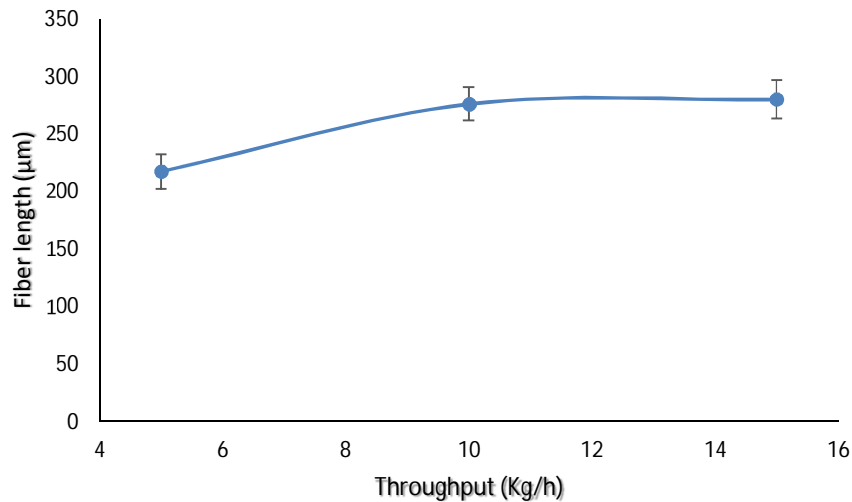


Figure 29: Influence of throughput on residual length of carbon fiber

This observation can be explained as follow. Low throughput leads to higher residence time and consequently higher shear energy. When throughput is increased from 5 to 10 kg/h, the residence time reduction lowers the amount of shear experienced and fibers length increases accordingly.

Yet, decreasing residence time (i.e. increase the output rate) beyond a certain point hindered heat transfer to the matrix leading in increased viscosity of the melt phase. This phenomenon competes with residence time and leads to lower fiber length than expected.

- **Influence of temperature on residual length of fibers**

As with output rate, a sharp increase in fiber length is observed between 240 and 270°C and then fiber length stabilizes until 300°C.

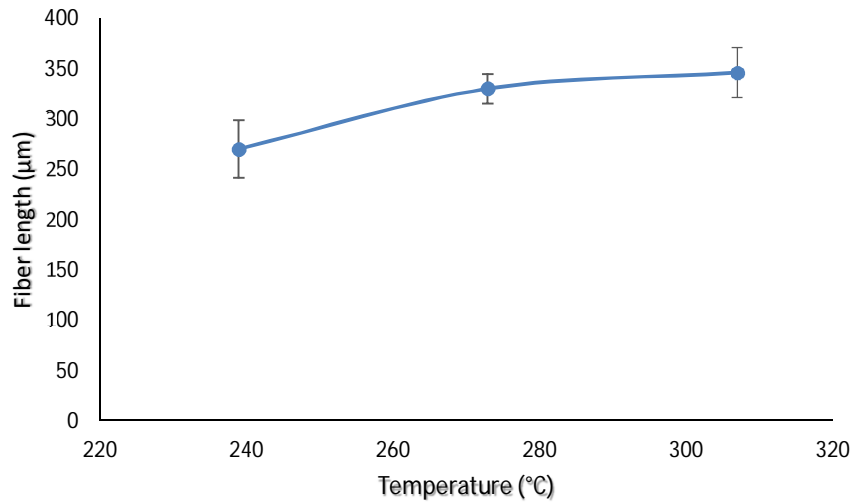


Figure 30: Influence of temperature on residual length of carbon fibers.

The melting temperature of polyamide 6 (PA6) is 221°C which means that 240°C is beyond its melting point.

However, the addition of fibers locally decreases the temperature eventually below its melting point. It results in an increase of the melt viscosity and hence higher shear.

At 270°C, the drop in temperature caused by the addition of fibers is not large enough to have a significant impact on melt viscosity and fibers are better preserved than at 240°C.

At 300°C, the melt viscosity is nearly the same than at 270°C. Consequently, no significant effects on fiber length are observed.

- **Influence of loading on residual length of fibers**

Figure 31 displays the impact of loading on residual length of fibers.

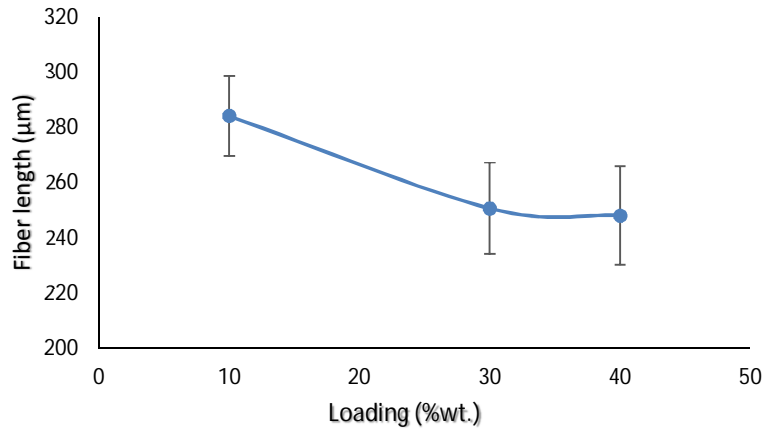


Figure 31: Influence of loading on residual length of carbon fibers

Fibers length decreases between 10 and 30% wt. It is assumed to be due to higher probability of fiber-fiber interactions leading to fibers breakage when the amount of fibers is increased. However, since at 30%wt., all fibers are presumably surrounded by other fibers. Further addition of fibers has limited impact toward fiber length at high fiber content.

- **Conclusion**

Table 7 recaps the optimized settings for TSE compounding of fibers.

Settings	Value
Output rate	10 kg/h
Screw speed	100 rpm
Temperature	270 °C

Table 7: TSE compounding optimized settings

4.2. Electrical and mechanical properties of composites

Previous section allowed us to determine optimized settings for the compounding of fibers by twin screw extrusion (TSE). These settings have been used for all samples investigated thereafter.

This section is divided in two parts. Herein, attention will be given to the effects of investigated fillers (carbon fiber PAN, carbon fiber PITCH and stainless steel fibers) on composites properties.

The first part of this chapter focuses on electrical properties. Percolation curves are displayed and discussed for each filler (carbon fiber PAN, carbon fiber PITCH and stainless steel).

In the second part the effects of selected fillers toward mechanical properties (i.e. tensile strength, elastic modulus, flexural strength and impact strength) are discussed.

▪ Volume resistivity

The dependence of volume resistivity on the filler content (i.e. percolation curves) in polyamide 6 (PA6) are shown in **Figure 32**.

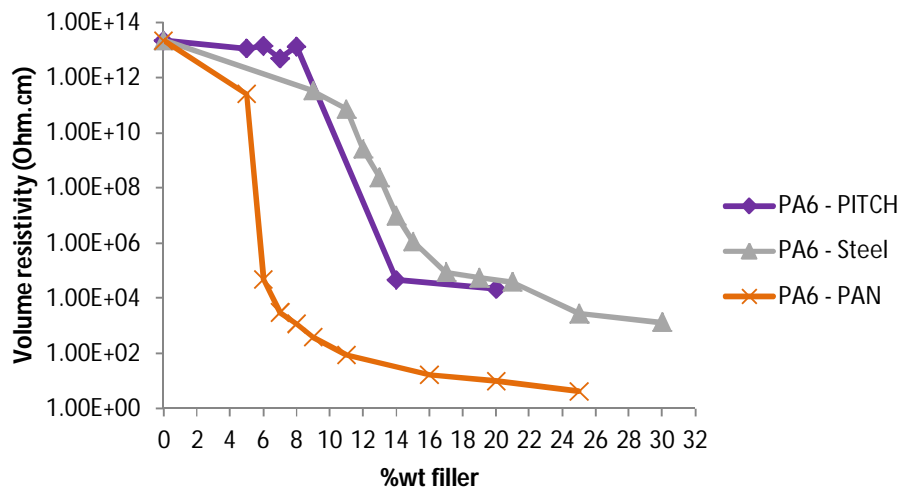


Figure 32: Dependence of volume resistivity on the filler content in polyamide 6.

For each curve, we observed that at low filler content the resistivity is similar to that of raw polymer. After a critical value (percolation threshold), resistivity subsequently drops and gets close to the conductive filler material (i.e. section 2.2 for individual filler electrical resistivity values).

Surprisingly, stainless steel fibers exhibit the lowest volume resistivity at high filler loading (beyond percolation threshold). This is presumably due to their high sizing content (25%vol. of sizing for stainless steel fibers versus 2% vol. for carbon fibers). This sizing which can easily be observed by electron microscopy (**Figure 33**) is assumed to produce an insulating layer around fibers.

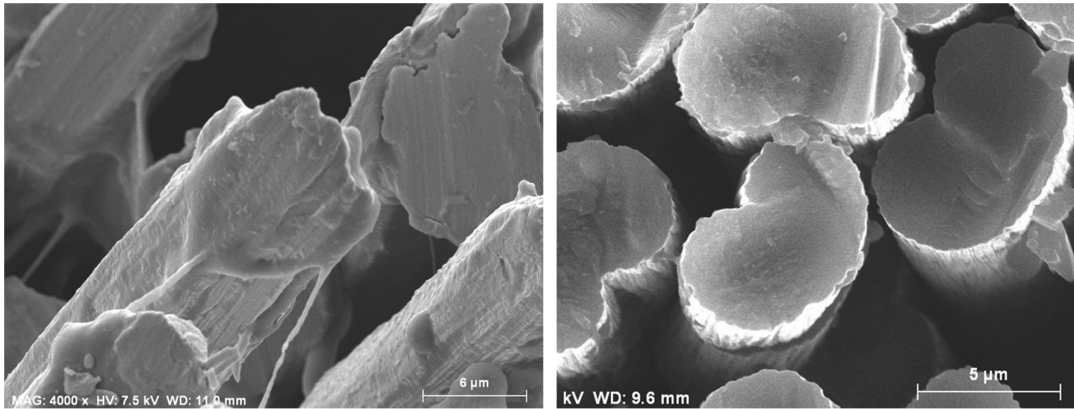


Figure 33: Scanning electron microscopy of raw stainless steel fibers (left) and carbon fibers PAN (right). Stainless steel high sizing amount can be seen by the less neat surface they exhibit when compared to carbon fibers.

In PA6, percolation thresholds are 5.5 %wt. (3.6 %vol.) for carbon fibers PAN; 11 %wt. (6 %vol.) for carbon fibers PITCH and 12 %wt. (2 %vol.) for stainless steel fibers.

Percolation threshold obtained for carbon fiber PAN are much lower than those observed elsewhere in literature when compounded by twin screw (i.e. 6.5% vol. [35] and 5% vol. [36]). This highlights the importance of the TSE optimization step performed previously in this work to maximize fibers lengths. This low percolation threshold is extremely interesting owing carbon fibers prices.

Carbon fibers PITCH exhibit unexpectedly high percolation threshold with values two times bigger than carbon fibers PAN whereas stainless steel fibers exhibits nearly two times lower percolation threshold (in volume fraction).

This can be explained as follow: Carbon fibers PITCH, owing their graphitic microstructure are more brittle (see **section 2.2**) and consequently more vulnerable to fibers degradation.

On the other hand, stainless steel fibers are extremely tough and accordingly less susceptible to degrade.

This was confirmed by optical microscopic analysis (**Figure 34**). Measured fibers length for carbon fibers PITCH are approximately 30% lower than carbon fibers PAN whereas stainless steel fibers exhibit fibers length roughly 30% higher than carbon PAN fibers.

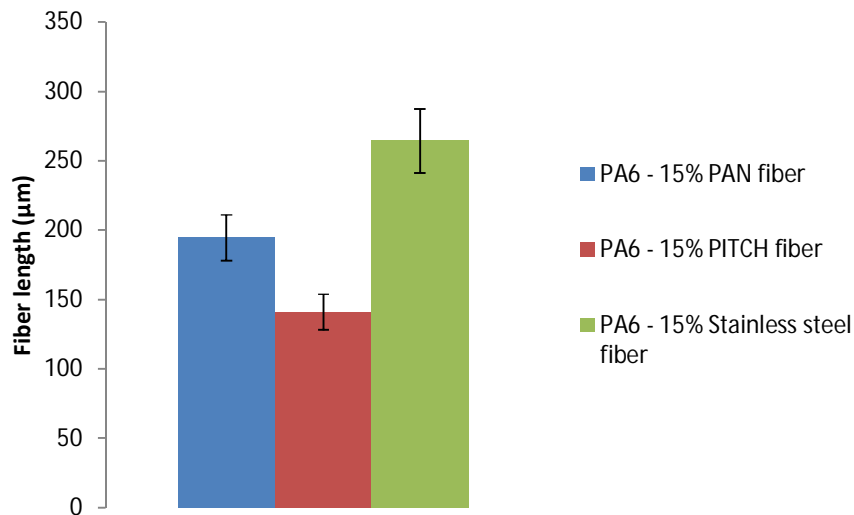


Figure 34: Comparison of Stainless steel, PITCH carbon fibers and PAN carbon fibers lengths. Samples were prepared using the same optimized compounding conditions and 15% wt. in PA6.

As explained in **section 2.1**, these differences in fibers length (i.e. aspect ratio) dramatically influence the percolation threshold.

Since matrix viscosity is expected to impact fibers lengths [37] further studies using polybutylene terephthalate (PBT) were performed to evaluate the influence of polymeric matrix toward percolation behavior. Results are displayed in **Figure 35**.

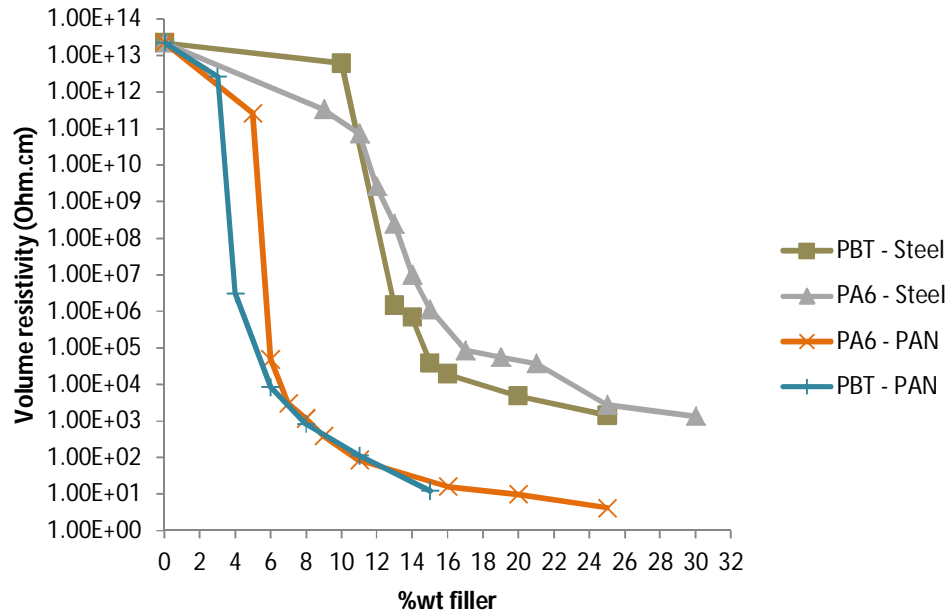


Figure 35: Percolation curves of carbon fibers PAN and stainless steel fibers in PBT and PA6 using optimized compounding settings.

It is observed (**Figure 35**) that percolation threshold in PBT are usually 1-2 % lower than in PA6 based composites for all tested fillers.

This may be explained by the lower viscosity of PBT matrix. This matrix viscosity was measured by the conventional melt flow index experiment and evidence a higher value of melt flow index, i.e. lower viscosity, for the PBT (**Figure 36**). Lower viscosity results in less shear during compounding and hence, higher fibers length (i.e. aspect ratio) as confirmed by microscopy analysis (**Figure 37**). Therefore, lower percolation threshold is observed for this PBT matrix (**Figure 37**).

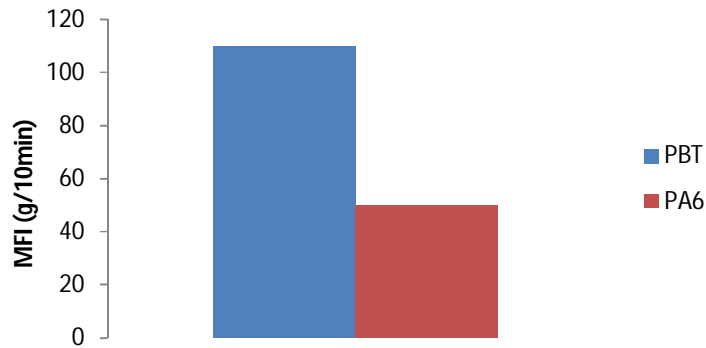


Figure 36: Melt flow index (viscosity) comparison between PBT and PA6. PBT exhibits much lower viscosity (higher MFI) than PA6. Tests were performed at 250°C and 10kg loading

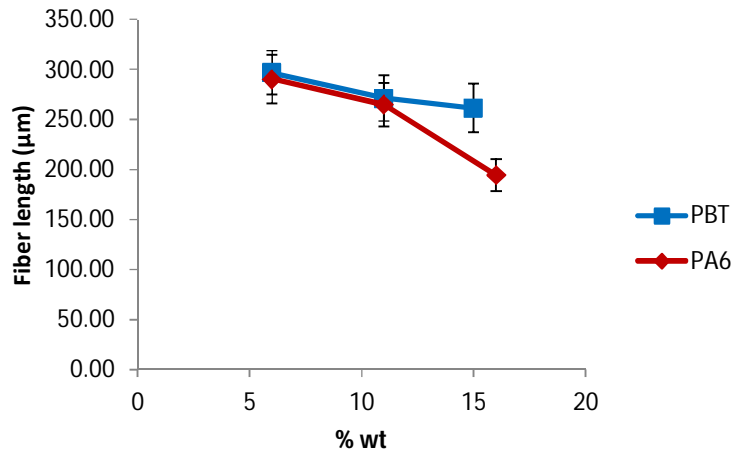


Figure 37: Comparison between carbon fibers length in PA6 and PBT. It is observed that carbon fibers exhibit higher length especially at higher loading.

Another hypothesis could be that lower viscosity may also lead to increased orientation of fibers during processing resulting in higher conductivity.

- **Yield strength**

The dependence of yield strength on the filler content in polyamide 6 (PA6) is shown in **Figure 38**.

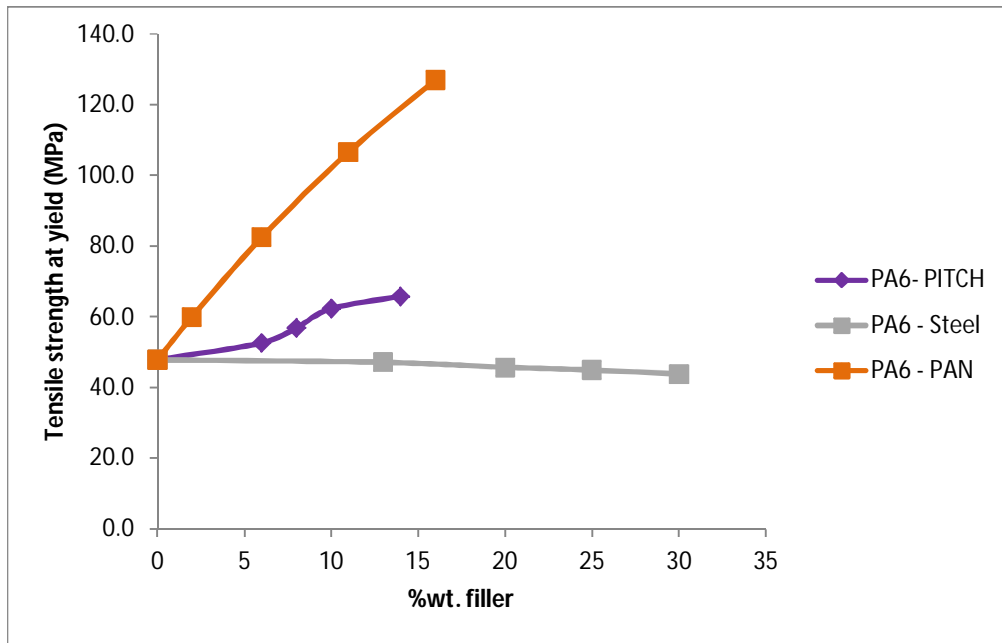


Figure 38: Influence of filler natures and content on yield strength of PA6

It can be seen that carbon fiber PITCH and PAN contribute significantly in increasing yield strength in PA6 whereas a slight degradation is observed for stainless steel fibers.

The absence of reinforcements observed in stainless steel fibers based composites are assumingly due to the poor adhesion of these fibers toward PA6 (**Figure 39**). [23] This is clearly evidenced by the SEM image of a fractured composite made of 15%wt. stainless steel fibers in PA6. It is easily seen that during fracture, stainless steel fibers are completely debounded from the matrix due to the lack of adhesion.

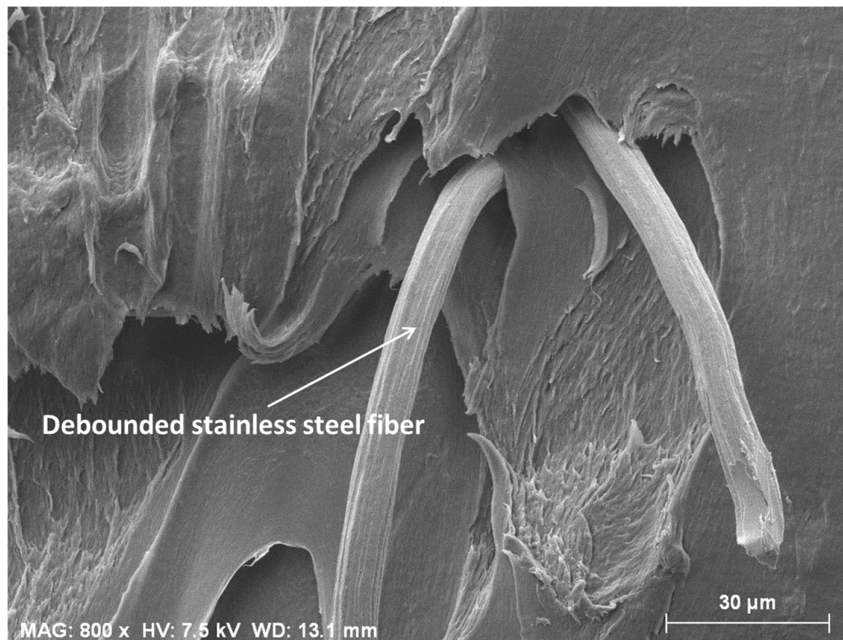


Figure 39: Scanning electron microscopy picture of a fractured composite made of 15%wt. stainless steel fibers in PA6.

PITCH carbon fibers provide much lower enhancement in yield strength than carbon fibers PAN. As explained in previous section, carbon fibers PITCH are more degraded during compounding. Subsequently, less reinforcement is observed (cf. **section 2.3**, critical fiber length).

- Rule of mixtures (RoM) applied to yield strength in carbon fibers

Hereafter a comparison between data observed in **Figure 38** and theoretical values predicted by the rule of mixtures equation (cf. **Equation 7**, section 2.3) is performed.

$$E_c = \eta_0 E_f V_f \left(1 - \frac{L_c}{L}\right) + E_m (1 - V_f) \quad \text{Equation 7}$$

According to literature [38], correction term η_0 , which depends on fiber orientation in composites, can be either 0.2 (random orientation), 0.375 (planar random orientation) or 1 (unidirectional orientation). (**Figure 40**)

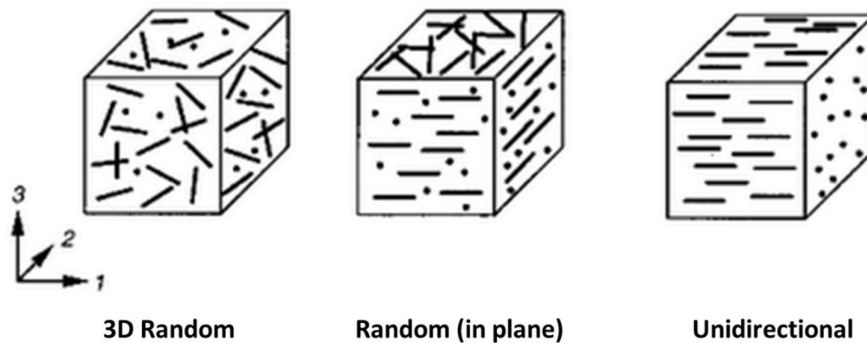


Figure 40: Schematic representation of fiber orientation in composite. Fibers can either orient randomly, randomly (in plane) or unidirectionally [38]

In order to estimate this term, optical microscopy analysis was performed on a carbon fiber based composite cross-section. This allows to evaluate fiber orientation and subsequently to estimate this correction term (**Figure 41**).

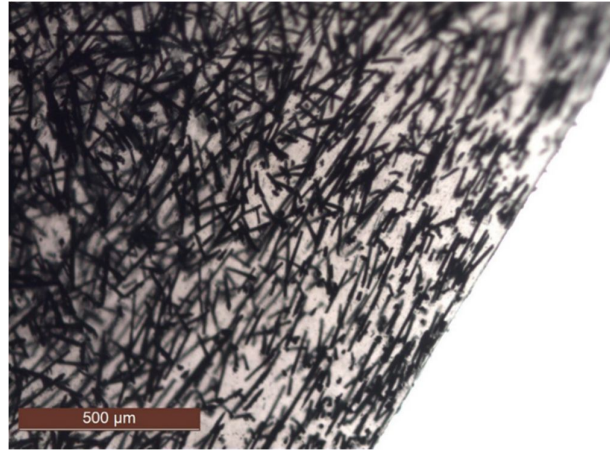


Figure 41: Optical micrograph of sample containing 10%wt. carbon fibers PAN in PA6.

It can be seen that fibers exhibit high orientation at sample edges whereas in the bulk, random orientation is observed. As a consequence, η_0 term should be roughly equal to 0.375 (i.e. planar random, cf. **section 2.3**).

Table 8 displays values of each terms displayed in Equation 7. The matrix used for this simulation is PA6, yield strength data are provided in datasheets mentioned **Annex A-2**, values for L_c are displayed in **section 2.3** (critical fiber length).

Filler	η_0	L for 10%wt. filler (μm)	$(1 - \frac{L_c}{L})$	Filler yield strength (Mpa)	Matrix yield strength (Mpa)
Carbon fiber PAN	0,375	265	0,63	4200	47.8
Carbon fiber PITCH	0,375	190	0,90	3430	47.8

Table 8: Values estimated and from datasheet used in RoM equation

Length at 10 %wt. was chosen as reference value because it is the median value for tested samples. Subsequently, fiber length variation is assumed to be minimized around this value.

As shown in **Figure 42**, a good agreement between experimental and computed data is observed.

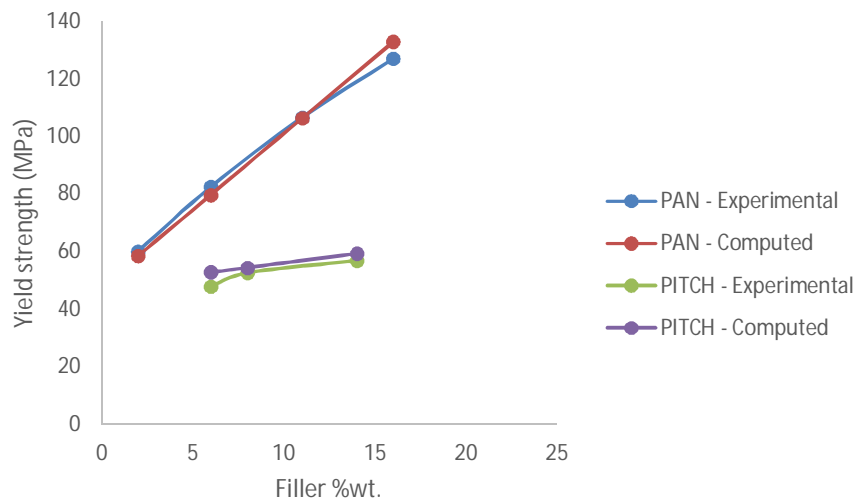


Figure 42: Comparison between computed values obtained from the RoM and experimental data.

For PAN carbon fibers, slight deviations from the RoM are observed at high and low filler content. This is presumably due to the variation of length with filler mass percentage (cf. **section 4.1**, influence of weight percentage).

PITCH carbon fibers also exhibits excellent fit to the model especially with increasing filler content. This is because, longer fibers are easily degraded than shorter ones [33]. Since PITCH carbon fibers are already severely degraded at low filler content, fiber length remains unchanged with increasing filler %wt.

- Effect of polymeric matrix

In **Figure 43**, the effect of matrix toward yield strength is displayed.

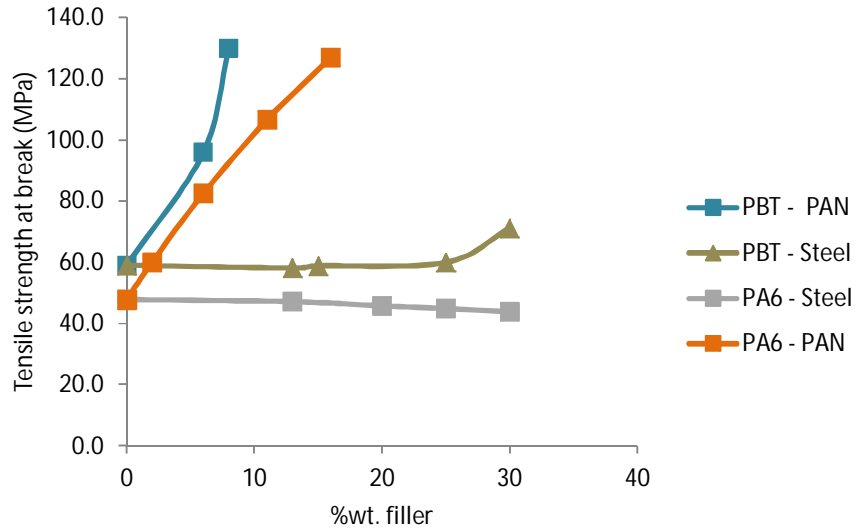


Figure 43: Influence of matrix toward yield strength

Stainless steel fibers still do not provide any reinforcements to PBT based composite whereas PAN carbon fiber are more efficient in PBT reinforcement, especially at higher filler content.

As observed for electrical resistivity, lower viscosity matrix (and hence, higher fiber lengths) allows fibers to be more efficient in reinforcing PBT resulting in higher enhancement in yield strength at high filler amount.

- **Flexural strength**

Similar trends as those observed for yield strength are measured for flexural strength (**Figure 44**).

In **Figure 44**, we observe that carbon fibers PAN provide high enhancement in flexural strength with value up to 200 MPa in PA6 and PBT. Carbon fibers PITCH also significantly enhance flexural strength and reach value up to 140 MPa whereas stainless steel fibers slightly alter composite properties.

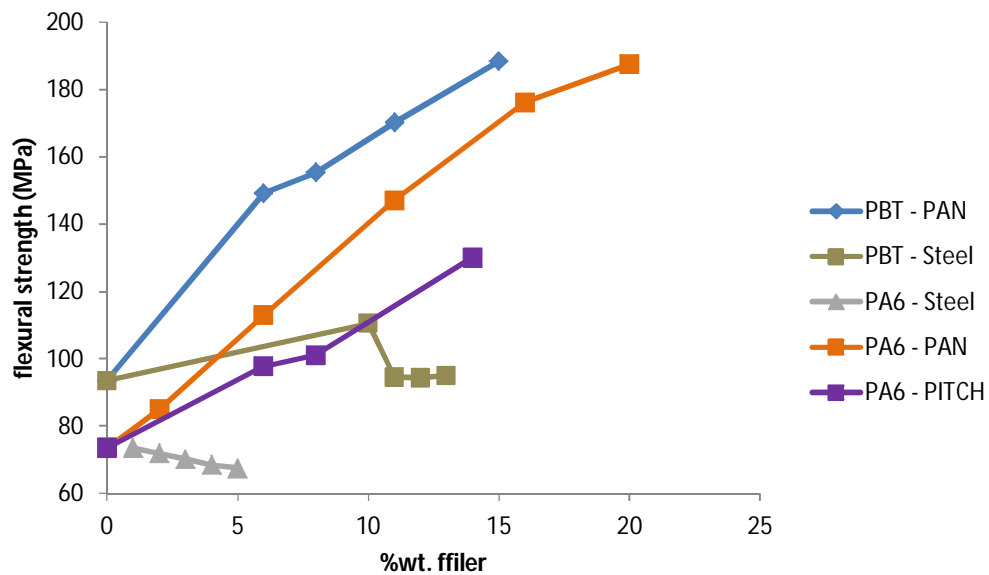


Figure 44: Influence of filler loading and nature on flexural strength of PA6 and PBT

- Elastic modulus

In **Figure 45**, results for both PITCH and PAN carbon fibers significantly enhance elastic modulus (i.e. rigidity) of composites. The enhancement is more pronounced than for yield and flexural strength.

Surprisingly, stainless steel fibers also significantly improve PAN elastic modulus.

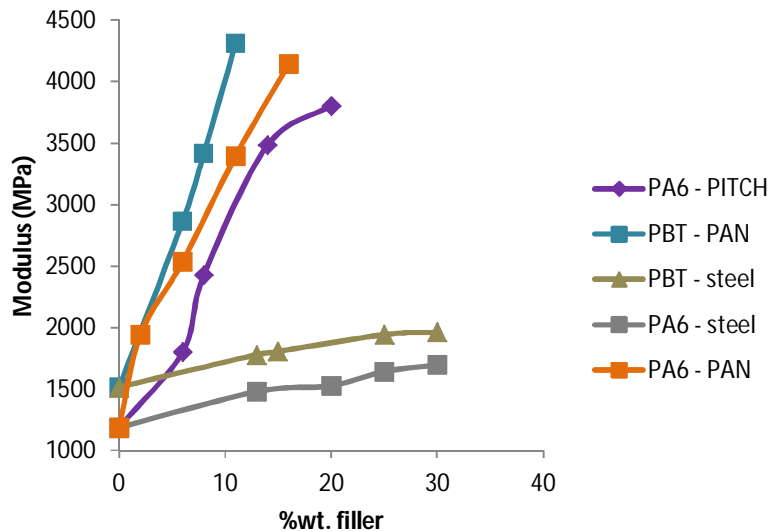


Figure 45 : Influence of filler loading (%wt.) and nature on elastic modulus in composite (PA6 and PBT)

Contrary to strength properties, modulus does almost not depend on the amount of adhesion between the filler and the polymer. This is because modulus tests are performed at relatively low stress. Subsequently, residual adhesion caused by weak Van der Waals interactions at the polymer – fiber interface is usually large enough to survive. [11] Another reason is that after compounding, during cooling, polymer shrinks more than fibers. This result in compressive forces as the polymer clenches around the fibers providing additional adhesion.

- Notched impact resistance

Figure 46 displays impact energy obtained for each tested composites.

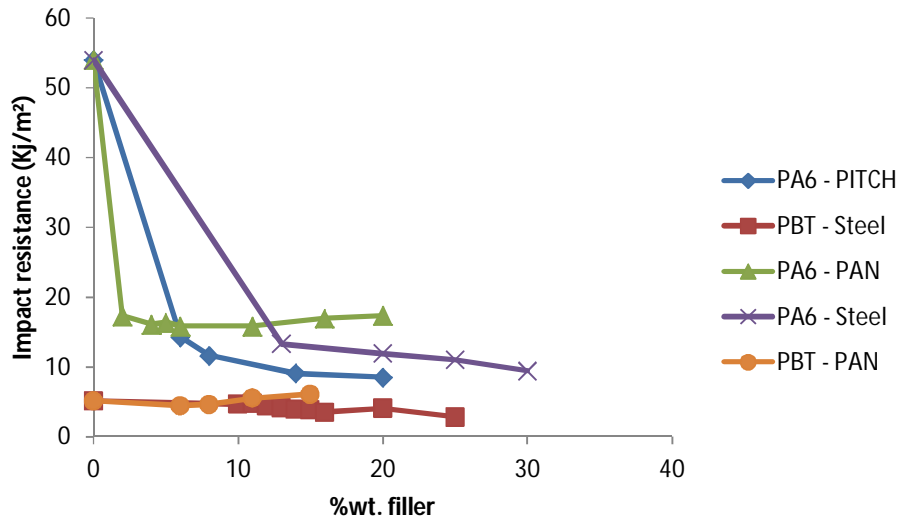


Figure 46: Influence of filler nature and loading on impact properties of composite (PA6 and PBT)

It can be seen in **Figure 46** that PAN carbon fiber exhibits the best performance when compared to PITCH carbon fibers and stainless steel fibers. Nevertheless, all tested composites exhibit poor impact resistance.

Impact resistance is extremely sensitive to irregularities and voids. Large and sharp particles such as fibers tend to increase stress concentration around them. As a consequence, when impact takes place, they act as flaws facilitating crack initiation and failure. This results in lower toughness in fiber reinforced composites. [38]

To explain the difference between PAN carbon fibers and other fibers, a brief discussion on failure mechanisms in composite will be performed hereafter.

Main mechanisms of failure in fiber reinforced polymer are fiber breakage, interfacial debonding and fiber pull-out.

Fiber breakage occurs when the applied stress exceeds fiber ultimate tensile strength resulting in fiber rupture. Fractured fibers may then be debonded from the matrix (interfacial debonding) and thereafter fibers start to be pulled out of their polymeric sockets (pull-out) if the applied stress is larger than the pull-out energy (**Figure 47**).

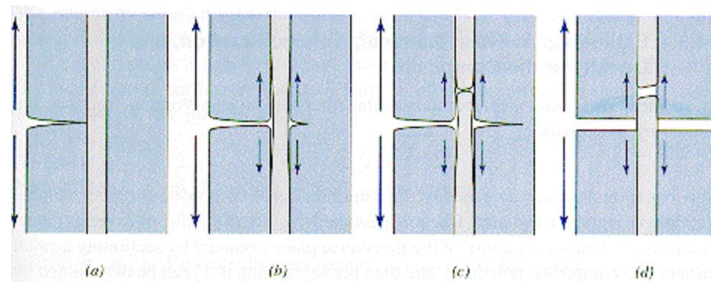


Figure 47: The matrix crack reaches the fiber (a), delamination occurs (b), fiber fracture is shown in (c) followed by fiber pullout in (d). [38]

The energy to completely pull-out a fiber is given by the following equation:

$$\Delta W = \int_0^{x_0} 2\pi r x \tau_i dx \quad \text{Equation 8}$$

Where r is the fiber radius, x the fiber pull-out length and τ_i the interfacial shear stress (**Figure 48**).

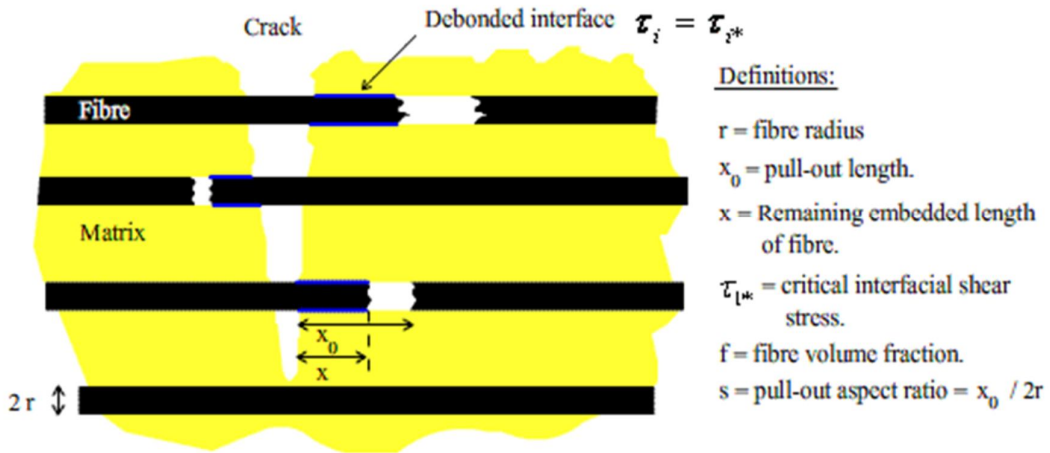


Figure 48: Detailed scheme representing complete pull-out mechanism.[39]

From **Equation 8**, it is easily seen that in order to increase pull-out energy, higher interfacial shear stress (which is proportional to the fiber-matrix adhesion) and pull-out length are necessary.

As results, if PAN carbon fiber based composite exhibits the highest toughness performances, it is because it combines higher fiber length (versus PITCH carbon fiber, **Figure 34**) and much higher adhesion (versus stainless steel fibers, **Figure 49**).



Figure 49: Stainless steel fibers fractured composite where complete fiber pull out of PA6 matrix is observed (left). PAN carbon fibers fractured composites where a fiber is still stuck into the PA6 matrix after rupture. This demonstrates a good adhesion of PAN carbon fibers (right).

4.3. Hybrid composite

In chapter 4.2, the effects of fillers addition toward mechanical and electrical properties of composites were studied. This allowed pinpointing benefits and drawbacks of each investigated fillers.

In this chapter, hybrid (i.e. containing at least two different fillers) composite are investigated.

In literature, hybrid combining fillers exhibiting very different properties are believed to provide original properties and possible synergistic effects [26].

The first investigated hybrid is made of stainless steel and carbon fibers. The purpose is to investigate possible synergistic effects on electrical and mechanical properties for future development in stainless steel based products for EMI applications.

Subsequently, in second section, hybrids containing carbon fibers and carbon black are studied. The objective is to investigate possible enhancement in mechanical and electrical properties when small amounts of fibers (i.e. 2%wt.) are used. Such hybrids are particularly interesting for Cabot, since it possibly enables to develop carbon black based conductive composite with enhanced mechanical performance, better fluidity and still cost competitive.

- **Stainless steel fiber (SF) – carbon fiber (CF) hybrid**

This section is divided into two parts. Firstly, electrical (volume resistivity) properties of tested hybrids are displayed. Subsequently, the second part is devoted to a discussion toward mechanical properties (i.e. yield strength, elastic modulus, flexural strength and impact resistance) of such hybrids.

SF-CF hybrids used PA6 as polymeric matrix and contain 21 %wt. of a blend with various fractions of SF and CF (PAN carbon fibers). Optimized compounding parameters discussed previously were used to manufacture each hybrid.

Since synergistic effects are more prone to appear after percolation of both fillers, 21%wt. was chosen as blend reference value because it allows being simultaneously at percolation for stainless steel fibers (i.e. 12%wt.) and carbon fibers (5.5%wt.) while keeping a safety margins in case of enhanced fibers degradation (i.e. higher percolation than expected). [40]

- **Volume resistivity**

Table 9 shows composition (%wt. and %vol.) of each tested blends.

%wt. carbon fiber PAN in the blend	%vol. carbon fiber PAN in the blend
0	38000
25	63,07
50	81,07
75	91,43
100	100

Table 9 : Composition of each blend in %wt. and %vol

The influence of blend composition on volume resistivity is displayed in **Figure 50**.

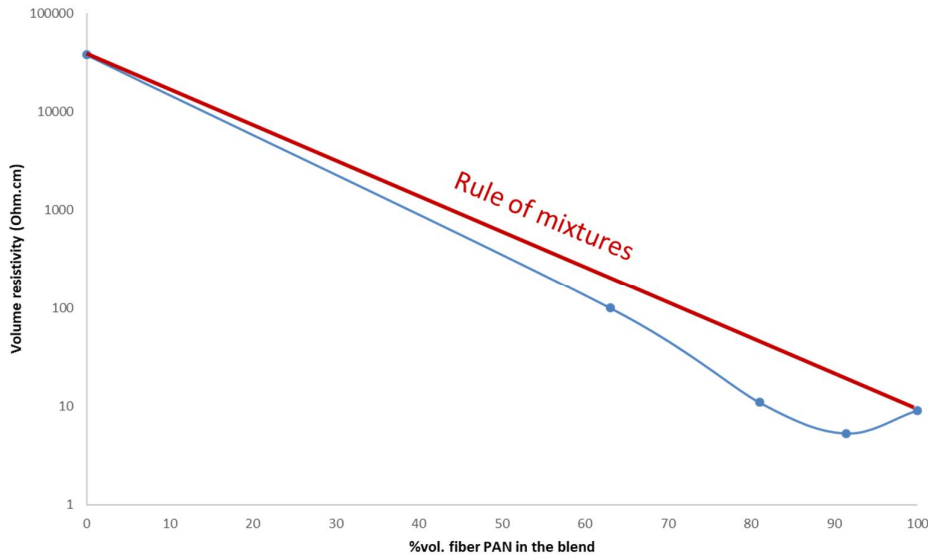


Figure 50: Volume resistivity of hybrids composite containing 21%wt. of a blend containing various amounts of stainless steel and carbon fibers. Polymeric matrix used is PA6.

It can be seen from **Figure 50** that positive synergistic effects occurred. This synergy results in lower volume resistivity than expected by rule of mixtures (red line) when both carbon fibers and stainless steel fibers are used.

Surprisingly, the largest effect appears at 91,43%vol. PAN fibers which corresponds roughly to 15%wt. of PAN carbon fibers and 5%wt. stainless steel fibers (i.e. below stainless steel fibers percolation) in the composite.

Similar trends were also observed elsewhere in literature [41] where conductivity of hybrid containing CB and CF in polypropylene displayed lower value than expected after percolation of both fillers and was attributed to loss of fibers orientation and low dispersion induced by CB particles.

In our case, stainless steel fibers owing their high flexibility and mass (density), may in a similar manner induce loss of carbon fibers orientation especially at high loading. On the other hand, at low loading, this flexibility is assumed to help interconnecting carbon fibers and consequently

substantially enhanced electrical conductivity and enhanced synergy is observed. (Figure 51)



Figure 51: picture of a burnt hybrid sample obtained by optical microscopy. SF are extremely flexible (i.e. wavy shape) when compared to carbon fibers (i.e. straight line).

Another explanation could be the enhanced shearing toward carbon fiber that stainless steel fibers induced. As results, when stainless steel fibers are present in larger amount, carbon fibers lengths are reduced and hence lower electrical conductivity.

- Yield strength

Figure 52 shows the evolution of yield strength with carbon fibers fraction.

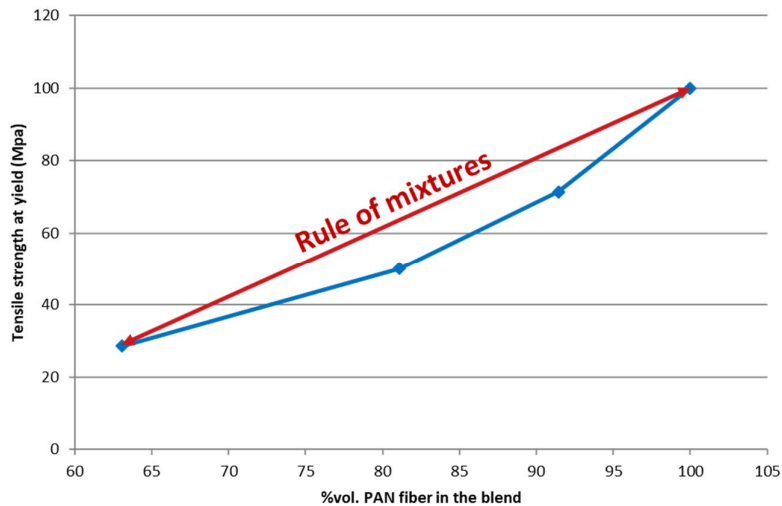


Figure 52: Evolution of yield strength of hybrids composite containing 21%wt. of a blend containing various amounts of stainless steel and carbon fibers. Polymeric matrix used is PA6

We saw in Chapter 4.2, that stainless steel fibers composites displayed poor mechanical properties owing low fibers adhesion to the matrix. **Figure 52** shows that significant reinforcement of stainless steel fibers based composite by addition of carbon fiber is possible.

This may be useful for manufacturing EMI shielding compounds exhibiting higher performances and lower density (since carbon fiber is lighter than stainless steel fiber).

However, reinforcement is not as high as expected using the rule of mixtures (red line in **Figure 52**). A possible explanation would be the enhanced carbon fibers degradation induced by fiber-fiber interactions (cf. **section 2.4**, Fiber compounding) due to stainless steel fibers addition (**Figure 53**).

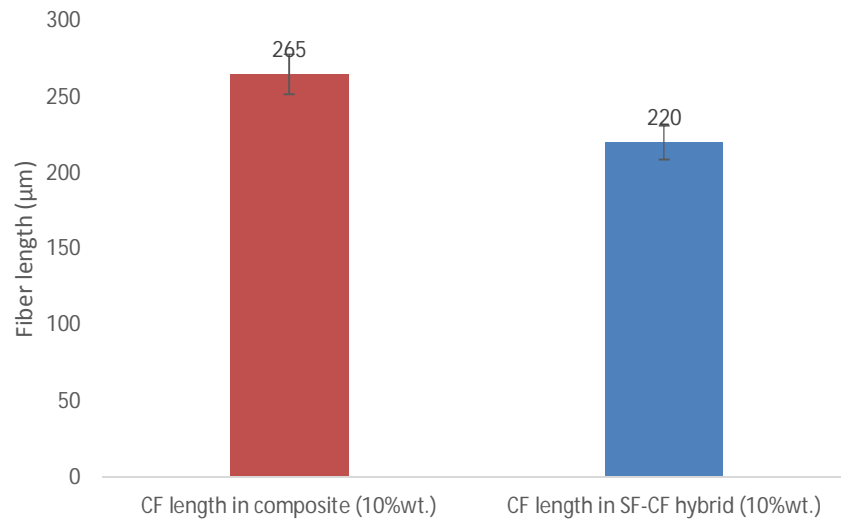


Figure 53: Fiber lengths comparison between samples containing 10%wt carbon fibers in hybrid and composite.

This was confirmed by optical microscopy analysis. Carbon fibers exhibits much lower length than in non-hybrid compounds. Furthermore, stainless steel fibers exhibit poor adhesion which also lowers hybrid composite mechanical properties.

- Flexural strength, elastic modulus and impact strength

Similar trends as those observed for yield strength are measured for flexural strength, elastic modulus and impact resistance (Figure 54, Figure 55 and Figure 56).

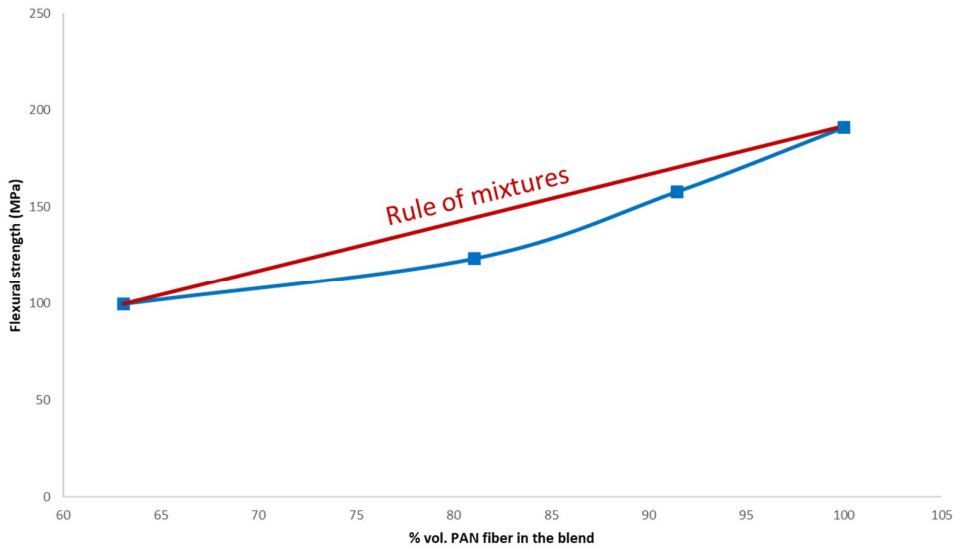


Figure 54: Evolution of flexural strength of hybrids composite containing 21%wt. of a blend containing various amounts of stainless steel and carbon fibers. Polymeric matrix used is PA6.

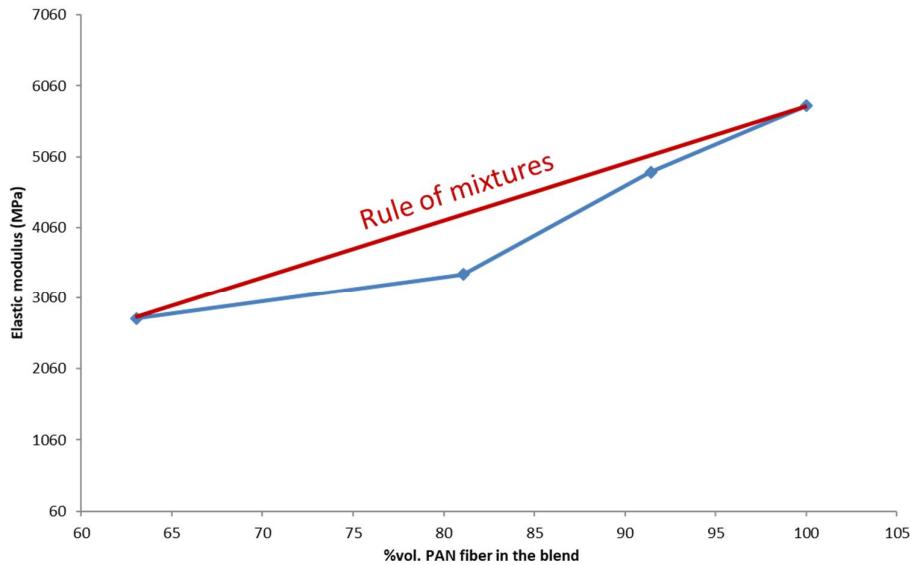


Figure 55: Evolution of elastic modulus of hybrids composite containing 21%wt. of a blend containing various amounts of stainless steel and carbon fibers. Polymeric matrix used is PA6.

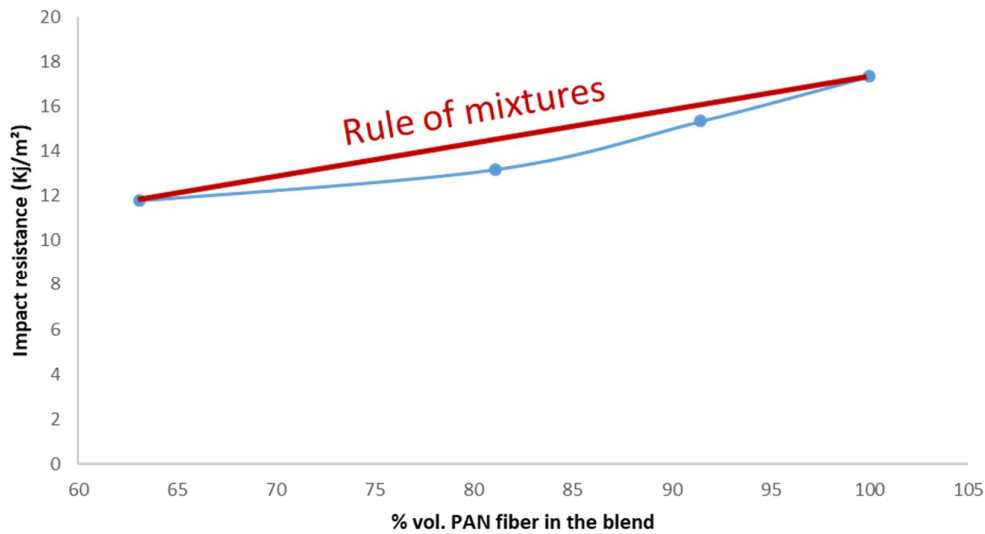


Figure 56: Evolution of impact energy of hybrids composite containing 21%wt. of a blend containing various amounts of stainless steel and carbon fibers. Polymeric matrix used is PA6.

▪ Conclusion

SF – CF hybrids displayed synergistic effects toward electrical conductivity. This was assumed to be due to stainless steel fibers flexibility which helps interconnecting carbon fibers and consequently substantially enhanced electrical conductivity. Furthermore, owing carbon fibers properties, resulting composites displayed significant reinforcement in strength and stiffness although slightly lower than expected due to fiber degradation.

Such composites are particularly interesting since it allows to benefits from the high EMI shielding efficiency of stainless steel and excellent mechanical properties from carbon fibers. Lastly, carbon fibers also help to reduce the weight of final composite.

- **Carbon black (CB) – carbon fiber (CF) hybrid**

In this chapter, the impact of small amount of carbon fiber PAN toward mechanical and electrical properties of a carbon black based composite is investigated. CB-CF hybrid contained 10%wt. CB and 2%wt. CF.

10%wt. CB in the hybrid was chosen for two reasons. Firstly, CB used in this work is a conductive grade (i.e. very fine particle) which severely increases melt viscosity when added resulting in dramatic increase in TSE torque (until eventually blocking the equipment). As a result, we weren't able to go higher than 10%wt. in CB loading without risking to damage the equipment. Hence, the first reason was technical considerations.

Secondly, according to a confidential Cabot internal report, percolation of such CB in these conditions occurs between 10-12%wt. This means that around 10%, slight addition of fibers may produce significant impact toward properties. This is this impact that we decided to investigate (i.e. bringing conductivity and mechanical enhancement at minimal fiber loading to reduce the fibers cost in such product).

Lastly, 2%wt fiber was the minimal amount of fiber that the TSE was able to measure so we decided to use this value since we weren't able to go lower.

- **Volume resistivity**

The resistivity results of carbon black composite (10%wt.) and CF-CB composite (2%wt. – 10%wt.) are displayed in **Figure 57**.

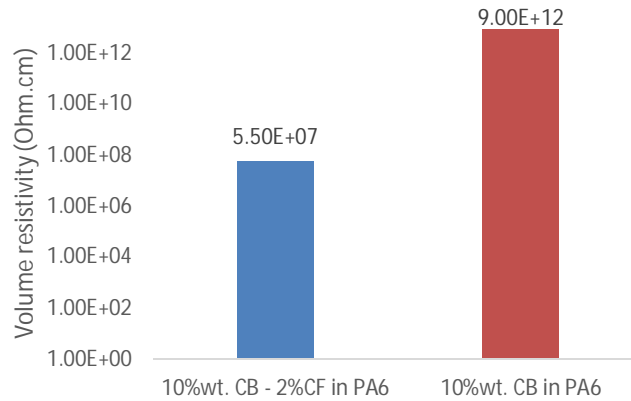


Figure 57: Influence of 2%CF PAN on the volume resistivity of a sample containing 10%CB. PA6 was used as polymeric matrix.

It can be seen that the addition of carbon fiber at small amount enhances by 5 order magnitude the volume resistivity. This phenomena can be explained as follows: When fibrous additives (i.e. carbon fibers) are combined with very fine particulates (i.e. CB), CF act as a long distance electron transporter [41]. On the other hand, CB create a local path witch interconnects fibers. Both phenomenon contribute to the formation of a continuous conductive network within the polymeric matrix resulting in this drop in resistivity.

- Yield and flexural strength - elastic modulus

Figure 58, Figure 59 and Figure 60 show the comparison between mechanical properties (i.e. yield and flexural strength, elastic modulus) of CB, CF and CB –CF composite.

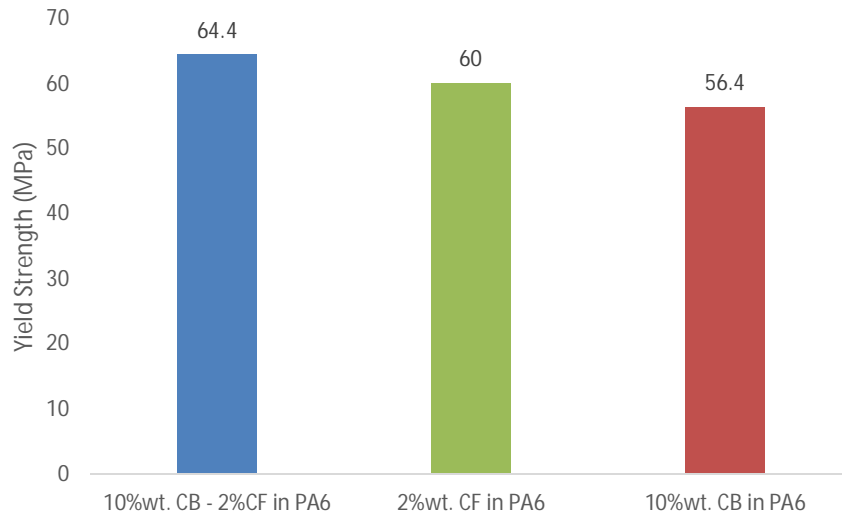


Figure 58: Influence of 2%CF PAN on the yield strength of a sample containing 10%CB. PA6 was used as polymeric matrix.

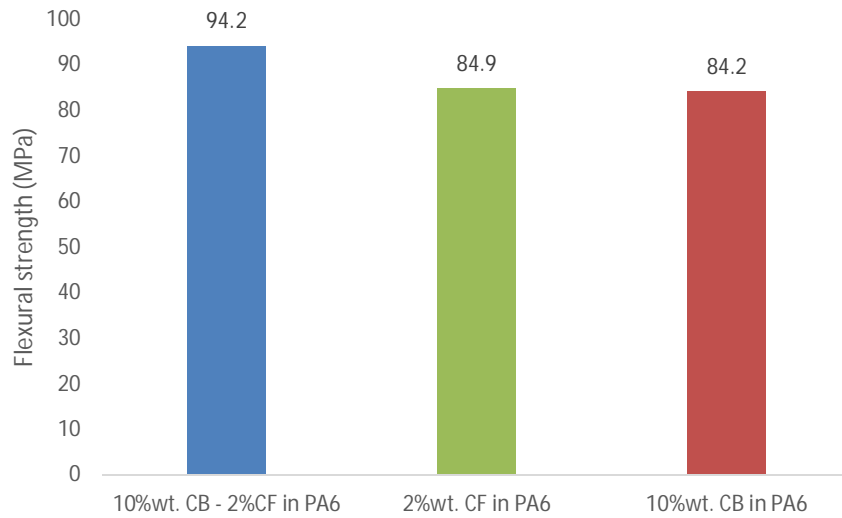


Figure 59: Influence of 2%CF PAN on the flexural strength of a sample containing 10%CB. PA6 was used as polymeric matrix.

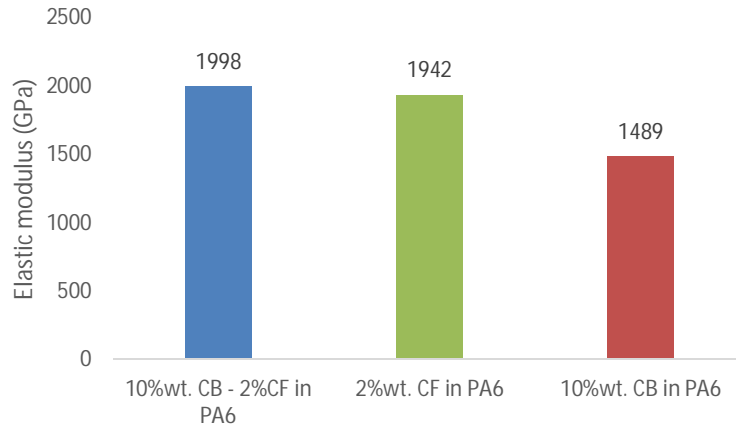


Figure 60: Influence of 2%CF PAN on the elastic modulus of a sample containing 10%CB. PA6 was used as polymeric matrix.

Besides significantly enhancing electrical conductivity, the addition of 2% carbon fibers also provides significant enhancement in mechanical properties (i.e. modulus and strength). Resulting composite are more strong and stiff than CF or CB based composite at 2% wt. and 10% wt. respectively. **(Figure 58, Figure 59 and Figure 60)**

However, as was the case for stainless steel fibers hybrids, reinforcement is lower than expected by the RoM. Very small particles such as carbon black significantly increase the melt viscosity **(Figure 61)**, as confirmed by lower melt flow index, resulting in higher shear during compounding and more fibers degradation.

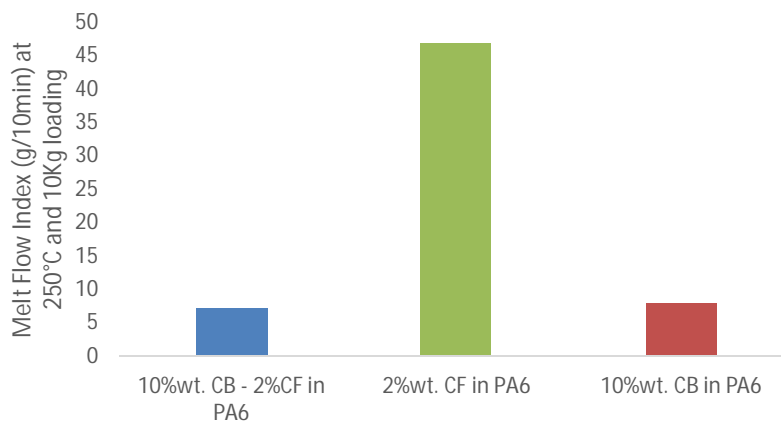


Figure 61: Melt flow index of samples containing 10% CB in PA6, 2%wt. in PA6 and a mix of 10%wt. CB and 2%wt. CF fibers.

Impact resistance is significantly reduced in CF-CB hybrids (**Figure 63**). This is because particles such as carbon fibers act as flaws where stresses concentrate.

Impact resistance is dramatically affected by any inhomogeneities, which act as crack initiator. Subsequently, the addition of fibers even at low levels severely degrades this value. [11]

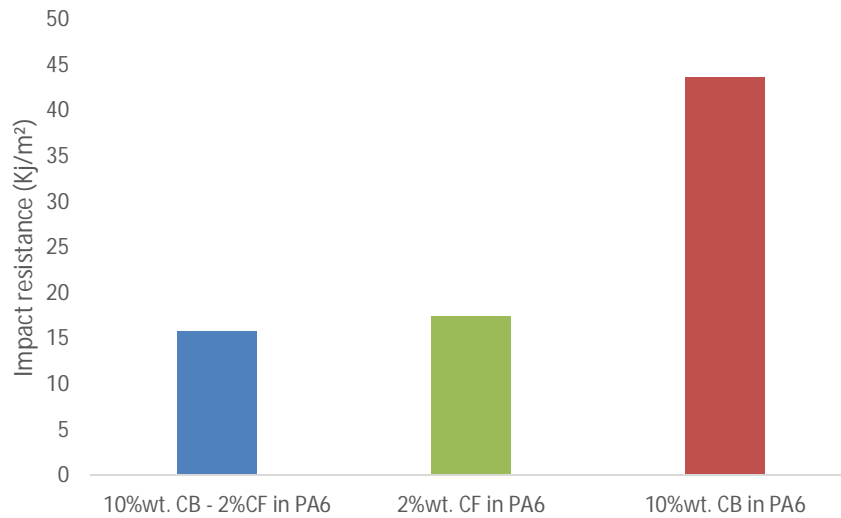


Figure 62: Influence of 2%CF PAN on the impact resistance of a sample containing 10%CB. PA6 was used as polymeric matrix

▪ **Conclusion**

CF-CB hybrids displayed significant enhancement in electrical conductivity. Furthermore, resulting hybrids exhibit enhanced strength and stiffness whereas toughness was reduced. Such hybrids would allow to catch up the lack of mechanical performance that suffers CB based composites.

Although, further studies are necessary to investigate deeper these effects which were not performed here due to technical limitations. For instance, one could vary the amount of CF and observe the impact of CB on fibers percolation.

5. Conclusion and perspectives

The first part of this work was devoted to the evaluation of TSE parameters impact toward fiber lengths and allowed to define optimized settings. It was shown that screw speed and fibers loading adversely affect fiber lengths whereas higher output rate and temperature help to preserve fibers.

Compounding by TSE using optimized parameters allowed manufacturing composite exhibiting enhanced mechanical properties and extremely low percolation threshold. Stainless steel fibers, carbon fibers PAN and carbon fibers PITCH displayed percolation at 2 %vol.; 3.6 %vol. and 6 %vol. respectively. These differences in percolation threshold are assumed to be due to the difference in filler aspect ratio after compounding.

Carbon fibers PAN provide composites exhibiting the best mechanical (i.e. stiffness and strength) and electrical performances (i.e. volume resistivity) among all tested fillers. This was attributed to their good adhesion to the matrix and relatively low degradation during compounding.

Carbon fibers PITCH, owing their graphitic microstructure resulting in high elastic modulus (i.e. brittleness) were more prone to fiber degradation and subsequently provided lower enhancement in composites performances than carbon fibers PAN.

Stainless steel fibers, besides being tougher than carbon fibers and consequently less degraded during compounding, displayed negative effects toward mechanical properties except for elastic modulus which is significantly enhanced. This was attributed to the poor adhesion of these fibers toward tested matrix. Unlike strength, modulus is almost not impacted by adhesion. Subsequently, fibers are usually more efficient in modulus than strength reinforcing. This trend was observed in all tested composites.

Matrix properties displayed significant impact toward fibers length and consequently on the efficiency of fillers to enhance composites properties.

Fibers in PBT displays better reinforcements and lower percolation threshold than in PA6, this was assumed to the lower viscosity of PBT, resulting in less shear during compounding and subsequently higher fiber lengths.

Optical microscopy analysis shown that TSE provides compounds exhibiting planar random orientation of fibers with length sensibly lower than the calculated critical length.

Orientation and length data were used to estimate correction terms in RoM equation. These terms were used to compute theoretical yield strength of carbon fibers reinforced PA6. Results were in good agreements with experimental data. This tool can therefore be used to predict compounds properties for future works.

RoM was not used for stainless steel fibers since it is only applicable to fillers exhibiting good adhesion toward matrix.

Impact resistance was low for each tested composites. It is presumably due to the relatively large size of fibers which increases stress concentration. Hence, fibers act as flaws and facilitate crack initiation and failure.

Based upon optical and electronic microscopy analysis, differences in impact resistance between carbon fibers PITCH and carbon fibers PAN were attributed to the difference in fiber lengths of both fillers whereas for stainless steel fibers, it was assumed to be due to the poor adhesion (i.e. low interfacial shear strength).

In the last part this work, two hybrids were investigated. The first hybrid was made of stainless steel and carbon fibers (SF-CF) whereas second hybrid contained carbon fibers and carbon black (CF-CB).

SF-CF hybrids displayed positive synergistic effects toward electrical properties. This was attributed to the high flexibility of stainless steel fibers which is assumed to help interconnecting carbon fibers and consequently substantially enhanced electrical conductivity.

Although the enhancement in mechanical properties was lower than expected, the addition of CF significantly increases strength, stiffness and toughness in SF-CF hybrids. This lower enhancement was attributed to fiber-fiber interactions between stainless steel fibers and carbon fibers resulting in lower average fiber lengths.

CF-CB hybrids displayed significant enhancement in electrical conductivity when 2%wt. CF is added (i.e. by five order of magnitude). This was explained by the difference in filler aspect ratio.

The addition of carbon fibers creates a long distance electron transporter whereas CB forms a local path which interconnects fibers. These phenomena contribute to the formation of a conductive network and result in a drop of the electrical resistivity.

The resulting hybrids exhibit enhanced strength and stiffness whereas toughness was significantly reduced. As already explained, impact resistance is very sensitive to any inhomogeneity. Hence, carbon fibers even at low loading, act as crack initiators and consequently severely affect impact properties.

All investigated properties have been demonstrated to dramatically depend upon fiber lengths. Subsequently, care must be taken in maximizing fiber length during compounding. Besides length, fiber adhesion was also of significant importance, since it dramatically affects strength and toughness.

As a consequence, there are still some researches to be done.

Since fiber length depends on compounding settings further investigation can be performed in order to optimize TSE settings. For instance, testing different side feeders position. It is clearly assumed that the later the fiber are injected into the TSE, the lower the residence time, and hence the higher the fiber length.

The use of plasticizers may also be interesting, since plasticizers lower the melt viscosity and subsequently lead to lower shear in the melt phase.

Screw profiles were not investigated in this work, but lower shearing profiles exist and may be used to preserve fibers.

A lot of work can be done in finding appropriate coupling agent that may enhance fibers adhesion. This would be the first step toward achieving composite exhibiting higher toughness.

Impact modifiers (i.e. rubber or elastomers added to absorb the energy of an impact) can also be investigated. Care must be taken since fibers may hindered their effects.[11]

Although the high sizing amount in stainless steel fibers contributes in preserving mechanical properties, it severely lowers electrical conductivity. Testing different sizing or surface treatments at lower loading would potentially dramatically enhance the electrical performance of SF.

Similarly, different amount of sizing for carbon fibers can be investigated. In this work, we choose to work with 2%wt. sizing in order to maximize electrical properties. But it is also possible to work with much higher sizing content (up to 8%wt) which could lead to significant strength and toughness enhancement.

Annexes


Annexes

- A-1: Popular fillers and application


	<u>Conductive Applications</u>	<u>Typical conductivity</u>	<u>Typical properties</u>	<u>System Cost</u>
Carbon Black	ESD, automotive	High and medium	Percolation curve, dusty, sloughing, influence on the polymer properties	0.4 – 2 Euros/kg
Carbon Fibers	Electronic, automotive, electrodes for fuel cell	High and medium	Good mechanical properties, light weight, clean, lower sloughing	From 0,5 to 4 Euros /kg
Graphite	Electrodes for fuel cell	High and medium	Conductivity, lubricant	From 0.6 to 3.5 Euros /kg
Multiwalled nanotubes	Clean room, automotive	High and Medium	Slight modification of polymer properties, clean, no sloughing	Between 1.7 and 6.8 Euros/kg
Metal	EMI Shielding	High	Conductivity, no sloughing, colourable	Between 6 and 10 Euros/kg
ICP / Polyaniline	ESD	Medium	Not clean, flatter percolation curve, dark green	Between 0.6 and 1.7 Euros/kg
Graphene	ESD, automotive	High	Conductivity, excellent mechanical properties, no sloughing	Between 5 and 20 Euros/kg (if 1%wt.)
IDP / Irgastat	Clean room	Low	Colourable, SR min 1E+10 Ohm/sq	Euros 1.4/kg
IDP / Stat-Rite	Clean room	Low	Colourable, SR min 1E+10 Ohm/sq	Between 2.4 and 4.0 Euros/kg

- A-2: Datasheets

- AC 4102 CHOPPED FIBER



Rev: 00/2017



AC 4102 CHOPPED FIBER TECHNICAL DATA SHEET

FIBER PROPERTIES

	English		Metric		Test Method
Tensile Strength	610	ksi	4200	MPa	ISO 10618
Tensile Modulus	34,8	Msi	240	GPa	ISO 10618
Elongation	1,8	%	1,8	%	ISO 10618
Density	0,064	Ft-lbs/in ³	1,76	kJ/m ³	ISO 10119

CHOPPED FIBER PROPERTIES

Chopped Fiber Properties					
Product Code	Applications	Fiber Lengths, mm	Typical Bulk Density (For 6mm cut lengths) (g/l)	Sizing Emulsion	Sizing content (%)
AC 4102	Thermoplastics-Special for PA and PBT	6	575	Polyamide based	1,5 - 2,0

DowAksa İleri Kompozit Malzemeler Sanayi LTD. ŞTİ.

Head Office: Miralay Şefik Bey Sok. Akhan No: 15 34437 Gümüşsuyu - İstanbul / TÜRKİYE
 T: +90(212) 251 45 00 • F: +90(212) 249 35 99
 Plant: Denizçalı Köyü Yalova - İzmit Yolu Cad. No: 34
 77600 Yalova / TURKEY
 T: +90 226 353 25 45
www.dowaksa.com • cfsales@dowaksa.com

- GRANOC® XN-80C-06S



Nippon Graphite Fiber Corporation

GRANOC Chopped Fiber, Milled Fiber**【Chopped Fiber】**

Grade	Length (mm)	Size *	Tensile modulus (GPa)	Tensile strength (MPa)	Thermal Conductivity (W/mK)	Electric Resistivity (10 ⁻⁸ Ωm)	Density (g/cm ³)
XN-100-03Z	3	No size	--	--	900	1.5	2.22
XN-100-06Z	6	No size	--	--	900	1.5	2.22
XN-80C-03S	3	Epoxy	780	3430	320	5	2.17
XN-80C-06S	6	Epoxy	780	3430	320	5	2.17
XN-60C-03S	3	Epoxy	620	3430	180	7	2.12
XN-60C-06S	6	Epoxy	620	3430	180	7	2.12
XN-P9C-03S	3	Epoxy	135	1900	5	25	1.80
XN-P9C-06S	6	Epoxy	135	1900	5	25	1.80
XN-P9C-06Z	6	No size	135	1900	5	25	1.80

【Milled Fiber】

Grade	Average Length (μm)	Size	Tensile modulus (GPa)	Tensile strength (MPa)	Thermal Conductivity (W/mK)	Electric Resistivity (10 ⁻⁶ Ωm)	Density (g/cm ³)
XN-100-05M	50	No size	--	--	900	1.5	2.22
XN-100-15M	150	No size	--	--	900	1.5	2.22
HC-600-10M	100	No size	--	--	600	2	2.22
HC-600-15M	150	No size	--	--	600	2	2.22
XN-P9C-10M	100	No size	135	1900	5	25	1.80
XN-P9C-15M	150	No size	135	1900	5	25	1.80

Nippon Graphite Fiber Corporation
 1, Fuji-cho, Hirohata-ku Himeji, Hyogo 671-1123 Japan
 Tel +81-79-256-7010 Fax +81-79-237-8427
 Website : www.ngfworld.com

- VULCAN® XCMAX™22



SPECIALTY CARBON BLACKS

VULCAN® XCMAX™ 22 Specialty Carbon Black



Product Highlights

VULCAN XCMAX 22 specialty carbon black is a highly conductive carbon black that achieves conductivity at the lowest loadings of traditional furnace blacks. Incorporating VULCAN XCMAX 22 specialty carbon black into formulations typically requires 50% of the required loading of other Cabot carbon blacks.

Key Applications

VULCAN XCMAX specialty carbon blacks are suitable for use in plastics where low loadings are required — typically where it is critical to maintain the underlying mechanical properties of the base polymer while protecting items against damage from electrostatic discharge (ESD). Examples of applications that may require ESD protection include:

- ◆ Automotive products such as fuel hoses, fuel inlets, and electrostatic coatings
- ◆ Industrial equipment and material (e.g. ATEX applications) to protect equipment, people, and processes from ESD hazards
- ◆ Appliances and electronics goods including packaging, mobile equipment, and other items sensitive to ESD damage

Performance Features

VULCAN XCMAX 22 specialty carbon black has a unique morphology allowing users to achieve target conductivity at much lower loadings than with other conductive carbon blacks while still maintaining the mechanical properties of the polymer. It features:

- ◆ High conductivity at relatively low loadings
- ◆ Physical cleanliness that enables end products to achieve a good aesthetic finish
- ◆ Processability in a variety of polymer systems

Typical Properties

PROPERTY	VALUE	TEST METHOD
Iodine Number	1360	ASTM D-1510
OAN (cc/100g)	320	ASTM D-2414
325 Mesh residue (PPM)	<100	ASTM D-1514
Density (kg/m ³)	190	ASTM D-1513

The data in the table above are typical test values intended as guidance only, and are not product specifications. Product specifications are available from your Cabot representative.

www.cabotcorp.com

- Zytel® ST7310 NC010

PRODUCT INFORMATION

DuPont™ Zytel® ST7301 NC010

NYLON RESIN

Product Information

ISO 1043: PA6-HI

Common features of Zytel® nylon resin include mechanical and physical properties such as high mechanical strength, excellent balance of stiffness and toughness, good high temperature performance, good electrical and flammability properties, good abrasion and chemical resistance. In addition, Zytel® nylon resins are available in different modified and reinforced grades to create a wide range of products with tailored properties for specific processes and end-uses. Zytel® nylon resin, including most flame retardant grades, offer the ability to be coloured.

The good melt stability of Zytel® nylon resin normally enables the recycling of properly handled production waste. If recycling is not possible, DuPont recommends, as the preferred option, incineration with energy recovery (-31kJ/g of base polymer) in appropriately equipped installations. For disposal, local regulations have to be observed.

Zytel® nylon resin typically is used in demanding applications in the automotive, furniture, domestic appliances, sporting goods and construction industry.

Zytel® ST7301 NC010 is a Super Tough, heat stabilised, lubricated polyamide 6 resin for injection moulding and extrusion. It offers outstanding impact resistance over a wide temperature and humidity range and high productivity.

General information	Value	Unit	Test Standard
Part Marking Code	>PA6-HI<	-	ISO 11469
Rheological properties	<i>dry / cond</i>	<i>Unit</i>	<i>Test Standard</i>
Viscosity number	150 / *	cm ³ /g	ISO 307, 1157, 1628
Moulding shrinkage, parallel	1.0 / *	%	ISO 294-4, 2577
Moulding shrinkage, normal	1.0 / *	%	ISO 294-4, 2577
Postmoulding shrinkage, normal, 48h at 80°C	0.1 / *	%	ISO 294-4
Postmoulding shrinkage, parallel, 48h at 80°C	0.1 / *	%	ISO 294-4
Mechanical properties	<i>dry / cond</i>	<i>Unit</i>	<i>Test Standard</i>
Tensile Modulus	1800 / 550	MPa	ISO 527-1/-2
Yield stress	48 / 29	MPa	ISO 527-1/-2
Yield strain	4 / 30	%	ISO 527-1/-2
Nominal strain at break	>50 / >50	%	ISO 527-1/-2
Flexural Modulus	1700 / 550	MPa	ISO 178
Flexural Stress at 3.5%	53 / 32	MPa	ISO 178
Tensile creep modulus, 1000h	* / 320	MPa	ISO 899-1
Charpy impact strength			ISO 179/1eU
23°C	N / N	kJ/m ²	
-30°C	N / N	kJ/m ²	
Charpy notched impact strength			ISO 179/1eA
23°C	80 / 120	kJ/m ²	
-30°C	17 / 18	kJ/m ²	
-40°C	18 / 17	kJ/m ²	
Izod notched impact strength			ISO 180/1A
23°C	60 / 95	kJ/m ²	
-30°C	14 / 15	kJ/m ²	
-40°C	15 / 13	kJ/m ²	
Ball indentation hardness, H 358/30	95 / -	MPa	ISO 2039-1
DS: Derived from similar grade			DS
Thermal properties	<i>dry / cond</i>	<i>Unit</i>	<i>Test Standard</i>
Melting temperature, 10°C/min	221 / *	°C	ISO 11357-1/-3
Temp. of deflection under load			ISO 75-1/-2
1.8 MPa	51 / *	°C	
0.45 MPa	95 / *	°C	
Thermal conductivity of melt	0.15	W/(m K)	-
Spec. heat capacity of melt	2600	J/(kg K)	-

Revised: 2015-01-30

Page: 1 of 9

To find out more, visit [DuPont Performance Polymers](#) or contact nearest DuPont location.

North America

Tel: +1 302 999-4592

Toll-Free (USA): 800 441-0575

Asia Pacific

Tel: +81 3 5521 8600


Europe/Middle East/Africa

Tel: +41 22 717 51 11



Copyright 2014 DuPont. The DuPont Oval Logo is a trademark or registered trademark of E.I. du Pont de Nemours and Company or its affiliates. All rights reserved.

- Ultradur® B4500

Product Information	Ultradur®	 BASF We create chemistry
	B 4500	
09/2016	PBT	

Product description

Medium-viscosity grade for the production of extruded cast films and thin-walled profiles and pipes.

Abbreviated designation according to ISO 1043-1: PBT
 CLASSIFICATION ACCORDING TO ISO 7792-1:
 Moulding Compound ISO 7792-PBT, E+F+MGHLN, 13-030

Product safety

Ultradur® melts are stable at temperatures up to 280°C and do not give rise to hazards due to molecular degradation or the evolution of gases and vapors. Like all thermoplastic polymers, however, Ultradur decomposes on exposure to excessive thermal stresses, e.g. when it is overheated or as a result of cleaning by burning off. At temperatures of > 290 °C can be emitted: carbon monoxide, tetrahydrofuran.
 Under special fire conditions traces of other toxic substances are possible. Formation of further decomposition and oxidation products depends upon the fire conditions.
 When Ultradur® is properly processed and there is adequate suction at the die no risks to health are to be expected. Further safety information see safety data sheet of individual product.
 Safety data sheet could be ask for at the Ultra-Infopoint under tel: 0621/60-78780 or fax:0621/60-78730.

Physical form and storage

Standard packaging includes the 25-kg-bag and the 1000 kg octabin (octagonal container). Other forms of packaging are possible subject to agreement. All containers are tightly sealed and should be opened only immediately prior to processing. Further precautions for preliminary treatment and drying are described in the processing section of the brochure. The bulk density is about 0,7 to 0,8g/cm³.
 Ultradur® can be stored for a longer period of time in dry, well vented rooms without causing problems in processing. Ultradur® should generally have a moisture content of less than 0,04% when being processed.
 In order to ensure reliable production, therefore, pre-drying should generally be the rule and the machine should be loaded via a closed conveyor system. Appropriate equipment is commercially available. Pre-drying is also for the addition of batches, e.g. in the case of inhouse pigmentation.
 In order to prevent the formation of condensed water, containers stored in unheated rooms must only be opened when they have attained the temperature prevailing in the processing area. This can possibly take a very long time. Measurements have shown that the interior of a 25-kg bag originally at 5°C had reached the temperature of 20°C in the processing area only after 48 hours.

Note

The data contained in this publication are based on our current knowledge and experience. In view of the many factors that may affect processing and application of our product, these data do not relieve processors from carrying out their own investigations and tests; neither do these data imply any guarantee of certain properties, nor the suitability of the product for a specific purpose. Any descriptions, drawings, photographs, data, proportions, weights etc. given herein may change without prior information and do not constitute the agreed contractual quality of the product. It is the responsibility of the recipient of our products to ensure that any proprietary rights and existing laws and legislation are observed. In order to check the availability of products please contact us or our sales agency.

▪ A-3: Profile screw configuration

SCREW CONFIGURATION NEW APV30 40:1

PROFILE 3

Screw profile for 1-2% CB in PA/PPO (CABELEC), Side-Feeder position 2, no kneading elements after CB addition

Nber	SCREW ELEMENT TYPE	ELEMENT LENGTH D	COMBINED LENGTH D	ELEMENT LENGTH mm	COMBINED LENGTH mm	SIZE in D/4 0,25	COMBINED LENGTH D/4	jam-02 section length (D)
1	FS 0.5D Lead	1,00	1,00	30,0	7,5	4	1,0	8,00
2	FS 1.0D Lead	1,00	2,00	30,0	37,5	4	5,0	
3	FS 1.0D Lead	1,50	3,50	45,0	82,5	6	11,0	
4	FS 1.0D Lead	1,50	5,00	45,0	127,5	6	17,0	
5	FS 1.0D Lead	1,50	6,50	45,0	172,5	6	23,0	
6	FS 1.0D Lead	1,50	8,00	45,0	217,5	6	29,0	
7	D/4 BLOCK 4° 30°	1,00	9,00	30,0	247,5	4	33,0	3,25
8	D/2 BLOCK 2° 60°	1,00	10,00	30,0	277,5	4	37,0	
9	D/2 BLOCK 2° 60°	1,00	11,00	30,0	307,5	4	41,0	
10	RFS	0,25	11,25	7,5	315,0	1	42,0	7,50
11	LFS 1.0 Lead	0,75	12,00	22,5	337,5	3	45,0	
12	LFS 1.0 Lead	0,75	12,75	22,5	360,0	3	48,0	
13	LFS 1.0 Lead	0,75	13,50	22,5	382,5	3	51,0	
14	LFS 1.0 Lead	0,75	14,25	22,5	405,0	3	54,0	
15	FS 1.0D Lead	1,50	15,75	45,0	450,0	6	60,0	
16	FS 1.0D Lead	1,50	17,25	45,0	495,0	6	66,0	
17	FS 1.0D Lead	1,50	18,75	45,0	540,0	6	72,0	
18	D/4 BLOCK 3° 30°	0,75	19,50	22,5	562,5	3	75,0	4,00
19	D/4 BLOCK 3° 30°	0,75	20,25	22,5	585,0	3	78,0	
20	D/4 BLOCK 3° 60°	0,75	21,00	22,5	607,5	3	81,0	
21	D/8 BLOCK 6° 60°	0,75	21,75	22,5	630,0	3	84,0	
22	D/8 BLOCK 4° 90°	0,50	22,25	15,0	645,0	2	86,0	
23	D/8 BLOCK 4° 90°	0,50	22,75	15,0	660,0	2	88,0	
24	FS 1.0D Lead	1,50	24,25	45,0	705,0	6	94,0	4,50
25	FS 1.0D Lead	1,50	25,75	45,0	750,0	6	100,0	
26	FS 1.0D Lead	1,50	27,25	45,0	795,0	6	106,0	
27	FDES	0,25	27,50	7,5	802,5	1	107,0	2,25
28	FDES	0,25	27,75	7,5	810,0	1	108,0	
29	FDES	0,25	28,00	7,5	817,5	1	109,0	
30	FDES	0,25	28,25	7,5	825,0	1	110,0	
31	FDES	0,25	28,50	7,5	832,5	1	111,0	
32	FDES	0,25	28,75	7,5	840,0	1	112,0	
33	FDES	0,25	29,00	7,5	847,5	1	113,0	
34	FDES	0,25	29,25	7,5	855,0	1	114,0	
35	RFS	0,25	29,50	7,5	862,5	1	115,0	
36	FS 1.0D Lead	1,50	31,00	45,0	907,5	6	121,0	11,00
37	FS 1.0D Lead	1,50	32,50	45,0	952,5	6	127,0	
38	FS 1.0D Lead	1,50	34,00	45,0	997,5	6	133,0	
39	FS 1.0D Lead	1,50	35,50	45,0	1042,5	6	139,0	
40	FS 1.0D Lead	1,50	37,00	45,0	1087,5	6	145,0	
41	FS 1.0D Lead	1,00	38,00	30,0	1117,5	4	149,0	
42	FS 1.0D Lead	1,00	39,00	30,0	1147,5	4	153,0	
43	FS DISCH SCREW	1,50	40,50	45,0	1192,5	6	159,0	
		40,50		1215		162 1215	Conveying : 31,00 Mixing : 9,50 40,50	1215,00

Side Feeder : 1st position = 13.5 D
Side Feeder : 2nd position = 23.5 D
Side Feeder : 3rd position = 28.5 D

SCREW ELEMENTS DESC.	APV CODE	LENGTH (D)	Number 1 screw	Number PROFILE	EN STOCK au 24/3/00
TWIN FEED SCREW 0.5D LEAD		1,0	1	2	
FEED SCREW (1.0D PITCH)	1.0D FS	1,0	3	6	
FEED SCREW (1.0D PITCH)	1.5D FS	1,5	15	30	
LONG FEED SCREW (1.5D PITCH)	0.75D LFS	0,75	4	8	
2*30°, D/2 BLOCK PADDLE	D/2 2*30°	1,0	2	4	
2*60°, D/2 BLOCK PADDLE	D/2 2*60°	1,0	2	4	
4*30°, D/4 BLOCK PADDLE	D/4 4*30°	1,0	1	2	
3*30°, D/4 BLOCK PADDLE	D/4 3*30°	0,75	2	4	
3*60°, D/4 BLOCK PADDLE	D/4 3*60°	0,75	1	2	
6*60°, D/8 BLOCK PADDLE	D/8 6*60°	0,75	1	2	
4*90°, D/8 BLOCK PADDLE	D/8 4*90°	0,5	2	4	
FLOW DIVISION ELEMENTS STRAIGHT	FDES	0,25	8	16	
REVERSE FEED SCREW	RFS	0,25	2	4	
DISCHARGE SCREW 0.75 LEAD	DS	1,5	1	2	
			T = 45	90	

▪ A-4: Compounding parameters and samples composition

Fiber length measurements

Process sheet		S0	S1	S2	S3	S4	S5	S6	S8	S9	S10	S11	S12	S13	S14	S15	S16
Ingredients																	
Doseur 1 - resin(s) in main entrance Zytel ST7301NC	wt% PA6	100,00	95,00	95,00	95,00	95,00	95,00	95,00	95,00	95,00	95,00	90,00	85,00	85,00	90,00	95,00	85,00
Doseur 2 - powder(s) in side-feeder Stainless steel fiber Carbon fiber	wt%SF	0,00	5,00	5,00	5,00	5,00	5,00	5,00	5,00	5,00	5,00	10,00	15,00	15,00	10,00	5,00	5,00
	wt%CF																
Verification	wt%	100,00	100,00	100,00	100,00	100,00	100,00	100,00	100,00	100,00	100,00	100,00	100,00	100,00	100,00	100,00	100,00
Process																	
SCREW PROFILE	#																
SCREW SPEED	rpm	300	300	100	500	300	300	300	100	100	500	300	300	100	100	100	100
TORQUE	%		31	38	27	40	22	26	56	39	34	33	36	57	57	58	61
OUTPUT	kg/h	10,0	10,0	10,0	10,0	15,0	5,0	10,0	10,0	10,0	10,0	10,0	10,0	10,0	10,0	10,0	10,0
DIE PRESSURE	bars		19	24	15	23	12	27	34	24	20	20	23	35	34	32	34
# of strands	#																
Brittleness of the strands																	
Side-Feeder SCREW SPEED	rpm	160	160	160	160	160	160	160	160	160	160	160	160	160	160	160	160
Side-Feeder SCREW Torque	%		10,0	11,0	10,0	10,0	11,0	11,0	15,0	10,0	10,0	14,0	17,0	22,0	16,5	10,0	10,0
SPECIFIC ENERGY INPUT(SF less)	kwh/kg	0,000	0,263	0,108	0,382	0,227	0,374	0,221	0,159	0,110	0,482	0,280	0,306	0,161	0,161	0,164	0,173
TEMPERATURE :		SET															
ZONE 2	°C	270	270	270	270	270	270	300	240	240	240	270	270	240	240	240	240
ZONE 3	°C	270	270	270	270	270	270	300	240	240	240	270	270	240	240	240	240
ZONE 4	°C	270	270	270	270	270	270	300	240	240	240	270	270	240	240	240	240
ZONE 5	°C	270	270	270	270	270	270	300	240	240	240	270	270	240	240	240	240
ZONE 6	°C	270	270	270	270	270	270	300	240	240	240	270	270	240	240	240	240
ZONE 7	°C	270	270	270	270	270	270	300	240	240	240	270	270	240	240	240	240
ZONE 8	°C	270	270	270	270	270	270	300	240	240	240	270	270	240	240	240	240
ZONE 9	°C	250	250	250	250	250	250	280	220	220	220	250	250	220	220	220	220
Melt Die	°C		268	269	268	270	267	315	238	239	238	270	272	238	233	236	236

Annexes

Process sheet		S0	S1	S2	S3	S4	S5	S6	S7	S8	S9	S10	S11	S12	S13
Ingredients															
Doseur 1 - resin(s) in main entrance															
Zytel ST7301NC	wt%	100,00	90,00	90,00	90,00	90,00	90,00	90,00	90,00	90,00	90,00	90,00	70,00	60,00	70,00
Doseur 2 - in side-feeder															
Carbon fiber PAN	wt%	0,00	10,00	10,00	10,00	10,00	10,00	10,00	10,00	10,00	10,00	10,00	30,00	40,00	30,00
Verification	wt%	100,00	100,00	100,00	100,00	100,00	100,00	100,00	100,00	100,00	100,00	100,00	100,00	100,00	100,00
Process															
SCREW PROFILE	#														
SCREW SPEED	rpm	300	300	100	500	300	300	300	100	100	100	500	300	300	100
TORQUE	%	25	36	47	32	47	24	29	37	61	62	37	21	23	40
OUTPUT	kg/h	10,0	10,0	10,0	10,0	15,0	5,0	10,0	10,0	10,0	10,0	10,0	10,0	10,0	10,0
DIE PRESSURE	bars	20	21	29	16	27	14	15	21	30	41	22	21	23	40
# of strands	#														
Brittleness of the strands															
Side-Feeder SCREW SPEED	rpm	160	160	160	160	160	160	160	160	160	160	160	160	160	160
Side-Feeder SCREW Torque	%	11	12	13	11	11	11	10	10	10	12	11	12	14	13
SPECIFIC ENERGY INPUT(SF less)	kwh/kg	0,212	0,306	0,133	0,453	0,266	0,408	0,246	0,105	0,173	0,176	0,524	0,178	0,195	0,113
TEMPERATURE :		SET													
ZONE 2	°C	270	270	270	270	270	270	300	300	240	240	240	270	270	240
ZONE 3	°C	270	270	270	270	270	270	300	300	240	240	240	270	270	240
ZONE 4	°C	270	270	270	270	270	270	300	300	240	240	240	270	270	240
ZONE 5	°C	270	270	270	270	270	270	300	300	240	240	240	270	270	240
ZONE 6	°C	270	270	270	270	270	270	300	300	240	240	240	270	270	240
ZONE 7	°C	270	270	270	270	270	270	300	300	240	240	240	270	270	240
ZONE 8	°C	270	270	270	270	270	270	300	300	240	240	240	270	270	240
ZONE 9	°C	250	250	250	250	250	250	280	280	220	220	220	250	250	220
Melt Die	°C	265	269	273	276	265	263	309	307	234	239	240	278	277	240

- Composites and hybrids

Process sheet														
		A0	A1	A2	A3	A4	A5	A6	B1	B2	B3_C3	B4	C2	C4
Ingredients														
Doseur 1 - resin(s) in main entrance														
Zytel ST7301NC	wt%	94,00	92,50	91,50	90,50	88,50	83,50	79,50	91,50	90,50	89,50	88,50	89,50	89,50
VXCmax22									4,00	5,00	6,00	7,00	10,00	4,00
Irganox 1098			0,50	0,50	0,50	0,50	0,50	0,50	0,50	0,50	0,50	0,50	0,50	0,50
Doseur 2 - powder(s) in side-feeder														
Carbon fiber	wt%	6,00	7,00	8,00	9,00	11,00	16,00	20,00	4,00	4,00	4,00	4,00	0,00	6,00
Process														
SCREW SPEED	rpm		100	100	100	100	100	100	100	100	100	100	100	100
TORQUE	%													
OUTPUT	kg/h		12,0	12,0	12,0	12,0	12,0	12,0	12,0	12,0	12,0	12,0	12,0	12,0
DIE PRESSURE	bars													
# of strands	#													
Side-Feeder SCREW SPEED	rpm		160	160	160	160	160	160	160	160	160	160	160	160
Side-Feeder SCREW Torque	%													
SPECIFIC ENERGY INPUT(SF less)	kwh/kg		0,000	0,000	0,000	0,000	0,000	0,000	0,000	0,000	0,000	0,000	0,000	0,000
TEMPERATURE :														
ZONE 2	°C		270	270	270	270	270	270	270	270	270	270	270	270
ZONE 3	°C		270	270	270	270	270	270	270	270	270	270	270	270
ZONE 4	°C		270	270	270	270	270	270	270	270	270	270	270	270
ZONE 5	°C		270	270	270	270	270	270	270	270	270	270	270	270
ZONE 6	°C		270	270	270	270	270	270	270	270	270	270	270	270
ZONE 7	°C		270	270	270	270	270	270	270	270	270	270	270	270
ZONE 8	°C		270	270	270	270	270	270	270	270	270	270	270	270
ZONE 9	°C		250	250	250	250	250	250	250	250	250	250	250	250
Melt Die	°C													

Process sheet		M1	M2	M3	M4	M5	M6	N1	N2	N3_N3	N4	N5
Ingredients												
Doseur 1 - resin(s) in main entrance	wt%											
Zytel ST7301NC		87,00	86,00	85,00	83,00	80,00	75,00	79,00	79,00	79,00	79,00	80,00
carbon fiber								21,00	15,00	6,00	0,00	10,00
Irganox 1098												
Doseur 2 - powder(s) in side-feeder	wt%											
Steel fiber		13,00	14,00	15,00	17,00	20,00	25,00	0,00	6,00	15,00	21,00	10,00
Process												
SCREW SPEED	rpm	200	200	200	200	200	200	200	200	200	200	200
TORQUE	%											
OUTPUT	kg/h	12,0	12,0	12,0	12,0	12,0	12,0	12,0	12,0	12,0	12,0	12,0
DIE PRESSURE	bars											
# of strands	#											
Side-Feeder SCREW SPEED	rpm	160	160	160	160	160	160	160	160	160	160	160
Side-Feeder SCREW Torque	%											
SPECIFIC ENERGY INPUT(SF less)	kwh/kg	0,000	0,000	0,000	0,000	0,000	0,000	0,000	0,000	0,000	0,000	0,000
TEMPERATURE :												
ZONE 2	°C	270	270	270	270	270	270	270	270	270	270	270
ZONE 3	°C	270	270	270	270	270	270	270	270	270	270	270
ZONE 4	°C	270	270	270	270	270	270	270	270	270	270	270
ZONE 5	°C	270	270	270	270	270	270	270	270	270	270	270
ZONE 6	°C	270	270	270	270	270	270	270	270	270	270	270
ZONE 7	°C	270	270	270	270	270	270	270	270	270	270	270
ZONE 8	°C	270	270	270	270	270	270	270	270	270	270	270
ZONE 9	°C	250	250	250	250	250	250	250	250	250	250	250

Annexes

Process sheet		7	8	9	10	11	12													
		Y1	Y2	Y3	Y4	Y5	Y6	X1	X2	X3	X4	X5	X6	Q9	Q10	Q11	P8	P9	P10	
Ingredients																				
Doseur 1 - resin(s) in main entrance PBT Zytel ST7301NC VXCmax22 Stainless steel Cabelec Ir98	wt%							96,000	95,000	94,000	93,000	86,000	80,000	98,000	97,000	96,000	91,000	90,000	89,000	
		95,00	94,00	93,00	92,00	86,00	80,00										9,00	10,00	11,00	
Doseur 2 - powder(s) in side-feeder PAN carbon fiber PITCH Carbon fiber	wt%													2,00	3,00	4,00				
		5,00	6,00	7,00	8,00	14,00	20,00	4,00	5,00	6,00	7,00	14,00	20,00							
Process																				
SCREW SPEED	rpm	100	100	100	100	100	100	100	100	100	100	100	100	100	100	100	100	100	100	
TORQUE	%																			
OUTPUT	kg/h	12,0	12,0	12,0	12,0	12,0	12,0	12,0	12,0	12,0	12,0	12,0	12,0	12,0	12,0	12,0	12,0	12,0	12,0	
DIE PRESSURE	bars																			
# of strands	#																			
Side-Feeder SCREW SPEED	rpm	160	160	160	160	160	160	160	160	160	160	160	160	160	160	160	160	160	160	
Side-Feeder SCREW Torque	%																			
SPECIFIC ENERGY INPUT(SF less)	kwh/kg	0,000	0,000	0,000	0,000	0,000	0,000	0,000	0,000	0,000	0,000	0,000	0,000							
TEMPERATURE :																				
ZONE 2	°C	270	270	270	270	270	270	250	250	250	250	250	250	270	270	270	250	250	250	
ZONE 3	°C	270	270	270	270	270	270	250	250	250	250	250	250	270	270	270	250	250	250	
ZONE 4	°C	270	270	270	270	270	270	250	250	250	250	250	250	270	270	270	250	250	250	
ZONE 5	°C	270	270	270	270	270	270	250	250	250	250	250	250	270	270	270	250	250	250	
ZONE 6	°C	270	270	270	270	270	270	250	250	250	250	250	250	270	270	270	250	250	250	
ZONE 7	°C	270	270	270	270	270	270	250	250	250	250	250	250	270	270	270	250	250	250	
ZONE 8	°C	270	270	270	270	270	270	250	250	250	250	250	250	270	270	270	250	250	250	
ZONE 9	°C	250	250	250	250	250	250	230	230	230	230	230	230	250	250	250	230	230	230	

Annexes

Process sheet		P1	P2	P3	P4	P5	P6	P7	P8	O1	O2	O3	O4	O5	O6	O7
Ingredients																
Doseur 1 - resin(s) in main entrance PBT Steel fiber Irganox 1098	wt%															
		95,00	94,00	93,00	92,00	91,00	89,00	85,00	80,00	88,00	87,00	86,00	85,00	84,00	80,00	75,00
										12,00	13,00	14,00	15,00	16,00	20,00	25,00
Doseur 2 - powder(s) in side-feeder carbon fiber	wt%															
		5,00	6,00	7,00	8,00	9,00	11,00	15,00	20,00							
Process																
SCREW SPEED	rpm	100	100	100	100	100	100	100	100	100	100	100	100	100	100	100
TORQUE	%															
OUTPUT	kg/h	12,0	12,0	12,0	12,0	12,0	12,0	12,0	12,0	12,0	12,0	12,0	12,0	12,0	12,0	12,0
DIE PRESSURE	bars															
# of strands	#															
Side-Feeder SCREW SPEED	rpm	160	160	160	160	160	160	160	160	160	160	160	160	160	160	160
Side-Feeder SCREW Torque	%															
SPECIFIC ENERGY INPUT(SF less)	kwh/kg	0,000	0,000	0,000	0,000	0,000	0,000	0,000	0,000	0,000	0,000	0,000	0,000	0,000	0,000	0,000
TEMPERATURE :																
ZONE 2	°C	250	250	250	250	250	250	250	250	250	250	250	250	250	250	250
ZONE 3	°C	250	250	250	250	250	250	250	250	250	250	250	250	250	250	250
ZONE 4	°C	250	250	250	250	250	250	250	250	250	250	250	250	250	250	250
ZONE 5	°C	250	250	250	250	250	250	250	250	250	250	250	250	250	250	250
ZONE 6	°C	250	250	250	250	250	250	250	250	250	250	250	250	250	250	250
ZONE 7	°C	250	250	250	250	250	250	250	250	250	250	250	250	250	250	250
ZONE 8	°C	250	250	250	250	250	250	250	250	250	250	250	250	250	250	250
ZONE 9	°C	230	230	230	230	230	230	230	230	230	230	230	230	230	230	230

Annexes

ProcA4:L32ess sheet		M9	M10	M11	A7	A8	A9	K0	K1	K2	K3
Ingredients											
Doseur 1 - resin(s) in main entrance	wt%										
Zytel ST7301NC		91,00	89,00	88,00	98,00	96,00	95,00	89,00	88,00	87,00	86,00
VXCmax22								9,00	10,00	11,00	12,00
Stainless steel		9,00	11,00	12,00							
Cabelec											
Ir98											
Doseur 2 - powder(s) in side-feeder	wt%										
Carbon fiber					2,00	4,00	5,00	2,00	2,00	2,00	2,00
Process											
SCREW SPEED	rpm	100	100	100	100	100	100	100	100	300	300
TORQUE	%										
OUTPUT	kg/h	12,0	12,0	12,0	12,0	12,0	12,0	12,0	12,0	8,0	8,0
DIE PRESSURE	bars										
# of strands	#										
Side-Feeder SCREW SPEED	rpm	160	160	160	160	160	160	160	160	160	160
Side-Feeder SCREW Torque	%										
SPECIFIC ENERGY INPUT(SF less)	kwh/kg	0,000	0,000	0,000	0,000	0,000	0,000	0,000	0,000	0,000	0,000
TEMPERATURE :											
ZONE 2	°C	270	270	270	270	270	270	270	270	270	270
ZONE 3	°C	270	270	270	270	270	270	270	270	270	270
ZONE 4	°C	270	270	270	270	270	270	270	270	270	270
ZONE 5	°C	270	270	270	270	270	270	270	270	270	270
ZONE 6	°C	270	270	270	270	270	270	270	270	270	270
ZONE 7	°C	270	270	270	270	270	270	270	270	270	270
ZONE 8	°C	270	270	270	270	270	270	270	270	270	270
ZONE 9	°C	250	250	250	250	250	250	250	250	250	250

***Bibliographic
references***

Bibliographic references

- [1] G. Kaur, R. Adhikari, P. Cass, M. Bown, and P. Gunatillake, "Electrically conductive polymers and composites for biomedical applications," *RSC Adv.*, vol. 5, no. 47, pp. 37553–37567, Apr. 2015.
- [2] W. Zhang, A. A. Dehghani-Sanij, and R. S. Blackburn, "Carbon based conductive polymer composites," in *Journal of Materials Science*, 2007, vol. 42, no. 10, pp. 3408–3418.
- [3] "Cabot Corporation | Specialty Chemicals and Performance Materials." [Online]. Available: <http://www.cabotcorp.com/>. [Accessed: 15-Jun-2017].
- [4] P. H. da S. L. Coelho, M. S. Marchesin, A. R. Morales, and J. R. Bartoli, "Electrical percolation, morphological and dispersion properties of MWCNT/PMMA nanocomposites," *Mater. Res.*, vol. 17, no. suppl 1, pp. 127–132, Aug. 2014.
- [5] T. Ishii, H. Sato, and R. Kikuchi, "Theory of hopping conduction by the path-probability method," *Phys. Rev. B*, vol. 34, no. 12, pp. 8335–8344, Dec. 1986.
- [6] T. Lee, W. Wang, and M. A. Reed, "Mechanism of Electron Conduction in Self-Assembled Alkanethiol Monolayer Devices," *Ann. N.Y. Acad. Sci.*, vol. 1006, pp. 21–35, 2003.
- [7] R. Fox, M. Barger, and V. Wani, "Electromagnetic shielding with conductive polymer composite materials," *doi.org*.
- [8] "Growth Opportunities in Carbon Fiber Market 2010-2015." [Online]. Available: http://www.lucintel.com/carbon_fiber_market.aspx. [Accessed: 15-Jun-2017].
- [9] M. E. Spahr and R. Rother, "Carbon Black as a Polymer Filler," pp. 1–31, 2016.
- [10] R. Blagus and L. Lusa, "Joint use of over- and under-sampling techniques and cross-validation for the development and assessment of prediction models," *BMC Bioinformatics*, vol. 16, no. 1, p. 363, Dec. 2015.
- [11] C. DeArmitt, "Functional Fillers for Plastics," in *Applied Plastics Engineering Handbook*, Elsevier, 2011, pp. 455–468.
- [12] "Nanotechnologies: 6. What are potential harmful effects of nanoparticles?" [Online]. Available: http://ec.europa.eu/health/scientific_committees/opinions_layman/en/nanotechnologies/1-2/6-health-effects-nanoparticles.htm. [Accessed: 15-Jun-2017].
- [13] S. Geetha, K. K. Satheesh Kumar, C. R. K. Rao, M. Vijayan, and D. C. Trivedi, "EMI shielding: Methods and materials-A review," *J. Appl. Polym. Sci.*, vol. 112, no. 4, pp. 2073–2086, May 2009.
- [14] D. D. L. Chung, "Materials for Electromagnetic Interference Shielding," *J. Mater. Eng. Perform.*, vol. 9, no. 3, pp. 350–354, Jun. 2000.
- [15] "Coming to carbon fiber: Low-cost mesophase pitch precursor : CompositesWorld." [Online]. Available:

- <http://www.compositesworld.com/news/coming-to-carbon-fiber-low-cost-mesophase-pitch-precursor>. [Accessed: 15-Jun-2017].
- [16] "The dawn of low-cost carbon fiber?: CompositesWorld." [Online]. Available: <http://www.compositesworld.com/blog/post/the-dawn-of-low-cost-carbon-fiber>. [Accessed: 15-Jun-2017].
- [17] J. Lehmann, S. Joseph, and Earthscan from Routledge., *Biochar for environmental management : science, technology and implementation*. .
- [18] F. G. Emmerich, "Evolution with heat treatment of crystallinity in carbons," *Carbon N. Y.*, vol. 33, no. 12, pp. 1709–1715, 1995.
- [19] *High-Performance Structural Fibers for Advanced Polymer Matrix Composites*. Washington, D.C.: National Academies Press, 2005.
- [20] "Materials Chemistry: Production carbon fibers." [Online]. Available: http://web.mit.edu/3.082/www/team2_f01/chemistry.html. [Accessed: 15-Jun-2017].
- [21] "Mechanics of Composites - Short Fibres." [Online]. Available: <http://www.mse.mtu.edu/~drjohn/my4150/class8/class8.html>. [Accessed: 13-Jun-2017].
- [22] K. TANAKA, Y. MASABE, and T. KATAYAMA, "Evaluation of Interfacial Properties for Carbon Fiber/ Polyamide Model Composites by Means of Single Fiber Pull-Out Test," *J. Soc. Mater. Sci. Japan*, vol. 58, no. 7, pp. 635–641, Jul. 2009.
- [23] D. M. BIGG, "6 – Properties and processing of short metal fibre filled polymer composites," in *Short Fibre–Polymer Composites*, 1996, pp. 144–167.
- [24] A. S. Virk, W. Hall, and J. Summerscales, "Modulus and strength prediction for natural fibre composites," *Mater. Sci. Technol.*, vol. 28, no. 7, pp. 864–871, Jul. 2012.
- [25] "Rule of Mixture for Elastic properties." [Online]. Available: [http://www.tech.plym.ac.uk/sme/mats333/rules of mixture.pdf](http://www.tech.plym.ac.uk/sme/mats333/rules%20of%20mixture.pdf). [Accessed: 15-Jun-2017].
- [26] "Estimations of composite materials properties [SubsTech]." [Online]. Available: http://www.substech.com/dokuwiki/doku.php?id=estimations_of_composite_materials_properties. [Accessed: 10-Jun-2017].
- [27] "Hot Melt Extrusion - Drug Manufacturing | Twin Screw Extruders." [Online]. Available: <http://www.particlesciences.com/news/technical-briefs/2011/hot-melt-extrusion.html>. [Accessed: 15-Jun-2017].
- [28] "Injection molding (ru)." [Online]. Available: <http://www.sopi-closures.com/ru/injection-molding-ru/>. [Accessed: 15-Jun-2017].
- [29] "Material properties for part design." [Online]. Available: http://www.dc.engr.scu.edu/cmdoc/dg_doc/develop/material/property/a2200002.htm. [Accessed: 15-Jun-2017].
- [30] M. Ashby, *Materials selection in mechanical design*. Butterworth-Heinemann,

- 2011.
- [31] K. D. Vernon-Parry, "Scanning electron microscopy: an introduction," *III-Vs Rev.*, vol. 13, no. 4, pp. 40–44, Jul. 2000.
- [32] "scanning electron microscope (SEM) | instrument | Britannica.com." [Online]. Available: <https://www.britannica.com/technology/scanning-electron-microscope>. [Accessed: 16-Jun-2017].
- [33] N. G. Karsli, A. Aytac, and V. Deniz, "Effects of initial fiber length and fiber length distribution on the properties of carbon-fiber-reinforced-polypropylene composites," *J. Reinf. Plast. Compos.*, vol. 31, no. 15, pp. 1053–1060, Aug. 2012.
- [34] "Shear thinning fluid Help for Non-Newtonian & Newtonian - Transtutors." [Online]. Available: <http://www.transtutors.com/homework-help/mechanical-engineering/fluid-mechanics/non-newtonian-fluids/shear-thinning-fluid/>. [Accessed: 08-Jun-2017].
- [35] C.-G. Zang, X.-D. Zhu, and Q.-J. Jiao, "Enhanced mechanical and electrical properties of nylon-6 composite by using carbon fiber/graphene multiscale structure as additive," *J. Appl. Polym. Sci.*, vol. 132, no. 19, p. n/a-n/a, May 2015.
- [36] X.-D. Zhu, C.-G. Zang, and Q.-J. Jiao, "High electrical conductivity of nylon 6 composites obtained with hybrid multiwalled carbon nanotube/carbon fiber fillers," *J. Appl. Polym. Sci.*, vol. 131, no. 20, p. n/a-n/a, Oct. 2014.
- [37] X. Huang and C. Zhi, *Polymer nanocomposites : electrical and thermal properties*. .
- [38] "Lecture 13." [Online]. Available: <https://www.slideshare.net/luyenkimnet/lecture-13>. [Accessed: 10-Jun-2017].
- [39] University of Cambridge, "DoITPoMS - TLP Library Mechanics of Fibre-Reinforced Composites - Single fibre pull out." [Online]. Available: https://doitpoms.admin.cam.ac.uk/tlplib/fibre_composites/fibre_pullout_derivation.php. [Accessed: 15-Jun-2017].
- [40] M. L. Clingerman, E. H. Weber, J. A. King, and K. H. Schulz, "Synergistic effect of carbon fillers in electrically conductive nylon 6,6 and polycarbonate based resins," *Polym. Compos.*, vol. 23, no. 5, pp. 911–924, Oct. 2002.
- [41] M. Drubetski, A. Siegmann, and M. Narkis, "Hybrid particulate and fibrous injection molded composites: Carbon black/carbon fiber/polypropylene systems," *Polym. Compos.*, vol. 26, no. 4, pp. 454–464, Aug. 2005.